



Universiteit
Leiden
The Netherlands

Next generation bacitracin: reimagining a classic antibiotic

Buijs, N.P.

Citation

Buijs, N. P. (2023, December 20). *Next generation bacitracin: reimagining a classic antibiotic*. Retrieved from <https://hdl.handle.net/1887/3674234>

Version: Publisher's Version

License: [Licence agreement concerning inclusion of doctoral thesis in the Institutional Repository of the University of Leiden](#)

Downloaded from: <https://hdl.handle.net/1887/3674234>

Note: To cite this publication please use the final published version (if applicable).



The development of
peptidomimetic inhibitors
of lipoprotein signal
peptidase II



Abstract

The global threat of antimicrobial resistance, particularly from Gram-negative bacteria, demands for the development of novel classes of antibiotics. Lipoprotein signal peptidase II (LspA) is an aspartyl protease with an essential role in lipoprotein processing in Gram-negative bacteria, making it a promising target for drug discovery. The recent publication of a crystal structure of LspA bound to the natural product globomycin has enabled the structure based design of new inhibitors. Here, we report the design, synthesis, and biological evaluation of the first peptidomimetic inhibitors of LspA. These findings provide new insights into structural features required for the development of LspA inhibitors as a novel class of anti-Gram-negative agents.

Introduction

Antimicrobial resistance (AMR) is a growing public health threat of global proportions. A recent study found that in 2019 there were 5 million deaths associated with AMR including 1.3 million deaths directly attributable to infections with drug-resistant bacteria.¹ While the rise of this 'silent pandemic' can partly be attributed to the mis- and overuse of antibiotics, the near empty pipeline of novel antimicrobial drugs is another major contributing factor to the restricted availability of effective antibiotics.² It is well established that infections due to Gram-negative bacteria are particularly more challenging to treat than Gram-positive infections.^{3–6} The presence of an outer membrane in Gram-negative bacteria acts as an additional barrier for antibiotics to pass before entering the cell to exert their effect. As such, the need for novel mechanisms that are capable of targeting Gram-negative strains is of the utmost importance.

The enzymes involved in bacterial lipoprotein processing are essential in many pathogenic Gram-negative bacteria and are not present in mammalian cells, making them interesting targets for antibiotics.^{7,8} Lipoprotein signal peptidase II (LspA) is an aspartyl protease that plays an essential role in the bacterial lipoprotein processing pathway (**Fig. 1**).⁹ Mature lipoproteins often possess an N-terminal cysteine residue that is post-translationally modified to bear one or more lipid tails.¹⁰ During lipoprotein maturation, LspA cleaves a transient membrane-anchoring signal peptide that initially localises lipoprotein precursors to the inner membrane prior to their lipidation.^{10,11} LspA recognises a consensus sequence in the signal peptide termed the 'lipobox' (most commonly L⁻³A⁻²G⁻¹C⁺¹) and cleaves at the N-terminal side of the lipidated cysteine residue, most often modified at its side chain with a diacylglycerol (DAG) group.^{10,12} Interference in the lipoprotein-processing pathway is lethal to many Gram-negative bacteria and presents a currently unexploited opportunity for antibacterial drug discovery.

Two natural products are known to selectively inhibit LspA: globomycin, produced by strains of *Streptomyces*, and myxovirescin, produced by *myxobacteria* (**Fig. 2**).^{13–15} It has been previously demonstrated that in Gram-negative bacteria, inhibition of LspA leads to a mis-localisation and accumulation of peptidoglycan-linked Braun's lipoprotein in the inner membrane, ultimately leading to bacterial cell death.^{16–18} Globomycin in particular is one of the best studied LspA inhibitors. It possesses antimicrobial activity against Gram-negative pathogens, demonstrating the viability of LspA inhibition as an effective antibacterial strategy.¹⁹ Recently, Caffrey and co-workers reported the first crystal structure of LspA.^{11,20} The co-crystal structure with bound globomycin revealed that it inhibits LspA by positioning

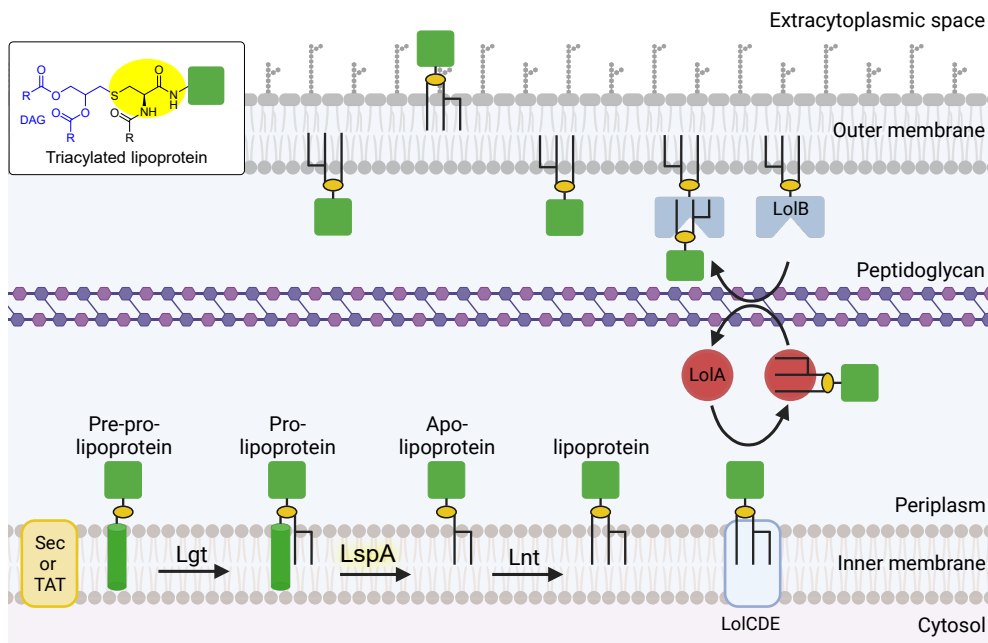


Figure 1. Lipoprotein post-translational processing pathway in Gram-negative bacteria. Pre-prolipoproteins enter the cytoplasmic membrane via the Sec or Tat pathways, with an N-terminal signal peptide (green cylinder) anchoring the lipoprotein domain (green square) to the membrane. The action of prolipoprotein diacylglyceryl transferase (Lgt) dagylates the pre-prolipoprotein through the side chain of a cysteine residue (yellow oval). LspA then recognises a consensus sequence in the prolipoprotein (LAGC*, where C* is the dagylated cysteine), leading to cleavage of the signal peptide at the amino end of C*. Some lipoproteins undergo further modification at the newly freed N-terminus by N-acyl transferase (Lnt), leading to further lipidation of the lipoprotein. The now mature lipoprotein is then trafficked to the outer membrane by the lipoprotein outer-membrane localisation (Lol) pathway. Made with Biorender.

its serine hydroxyl moiety in the active site of LspA, within hydrogen bonding proximity of the two catalytic aspartic acid residues.¹¹

These new structural insights have renewed interest in LspA as a novel target for antibiotic development. Aspartyl proteases are established drug targets including in the treatment of hypertension, malaria, and HIV.^{21–27} The development of aspartyl protease inhibitors for these

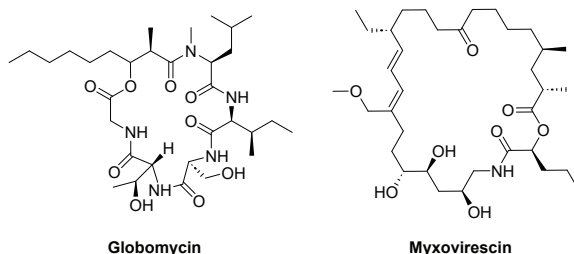


Figure 2. The chemical structures of the natural product LspA inhibitors globomycin and myxovirescin.

indications generally started with the design of peptidomimetic inhibitors inspired by the natural substrate sequences recognised by the protease. Many such peptidomimetic inhibitors contain a non-cleavable moiety designed to mimic the tetrahedral transition state of the proteolysis reaction (**Fig. 3**).²⁶ Despite the clinical success of aspartyl protease inhibitors in the diseases mentioned above, there are currently no clinically used antibiotics that are aspartyl protease inhibitors. Inspired by these successes, we chose to apply a similar peptidomimetic approach with the goal of developing novel inhibitors of LspA with antibacterial activity.

Herein, we report the design and synthesis of a panel of novel peptidomimetic inhibitors of LspA. The *in vitro* activity of these compounds as inhibitors of LspA was evaluated using a fluorescence resonance energy transfer (FRET) assay. Furthermore, the antibacterial activities of these compounds were also assessed against a panel of Gram-negative bacteria.

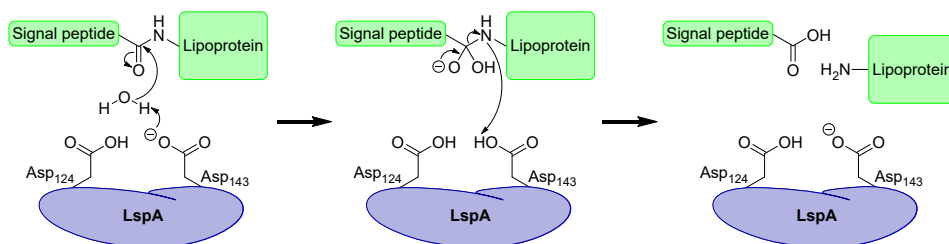


Figure 3. Schematic representation of LspA-catalysed signal peptide cleavage in bacterial lipoprotein processing. The proteolysis reaction proceeds via a tetrahedral transition state intermediate.

Results and Discussion

Synthetic chemistry

Our rational design approach towards the preparation of peptidomimetic inhibitors of LspA focussed on the inclusion of four distinct classes of non-cleavable moieties that have been successfully applied in the development of inhibitors of other aspartyl proteases.^{21,22,25,27,28} These are: hydroxymethylcarbonyl (HMC), statin (STA), reduced amide (RA), and difluoroketone (DFK) (**Fig. 4**). The HMC, STA and DFK groups have the potential to serve as tetrahedral transition state isosteres when used in aspartyl protease inhibitors. In addition to HMC, STA and DFK, the RA moiety was also explored, and these non-cleavable motifs were incorporated into peptides based on the conserved sequence of amino acid residues found in the lipobox of the signal peptide (LAGC*). LspA substrate sequence analysis has previously revealed that two serine residues at the C-terminal side of the lipobox are moderately conserved and well recognized by LspA.^{10,11} Accordingly, our peptidomimetic strategy initially focussed on the use of hexapeptides comprising the sequence Leu-Ala-X-Cys*-Ser-Ser where X is a non-

cleavable motif (**Fig. 4**). To increase the synthetic accessibility and to investigate the role of cysteine lipidation, the diacylglycerol motif, found in the natural substrate, was replaced with the simpler hydrophobic octyl and benzyl moieties. Also, in order to better resemble the natural peptidic substrate, the peptidomimetics were all synthesised as C-terminal amides, and N-terminal acetamides.

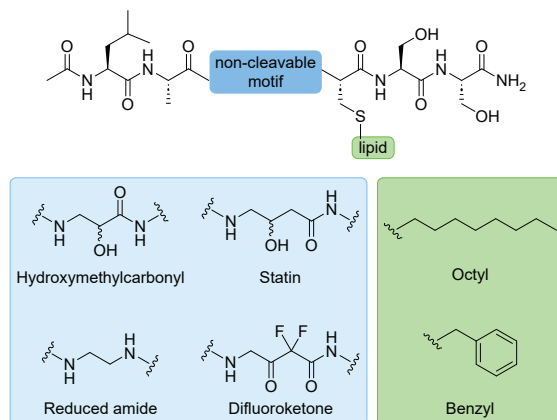
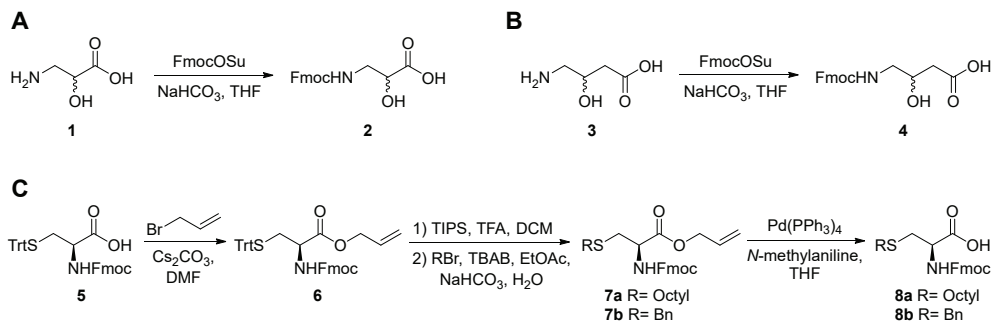


Figure 4. Overview of non-cleavable motifs and lipids utilised in the LspA peptidomimetic design strategy.

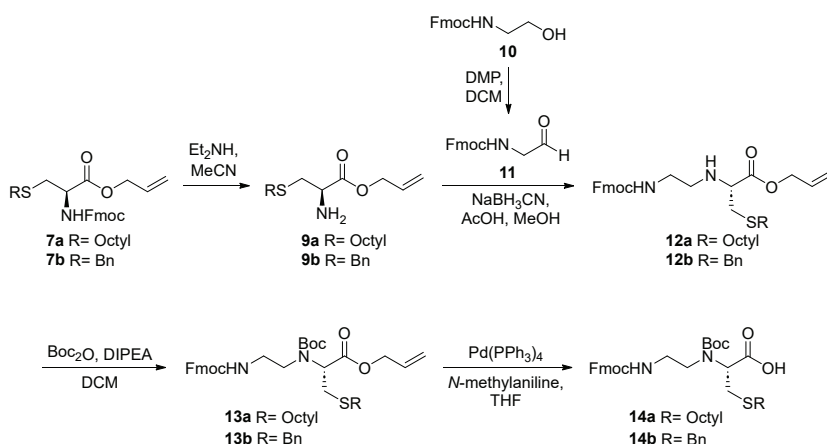
The non-cleavable motifs and lipidated cysteines were synthesised as Fmoc protected building blocks to facilitate their subsequent incorporation into the peptidomimetics through the use of solid-phase peptide synthesis (SPPS). The hydroxymethylcarbonyl containing Fmoc amino acid **2** was prepared from readily available 3-amino-2-hydroxypropanoic acid **1**, through simple Fmoc protection of the free primary amine (**Scheme 1A**). A similar approach was equally successful in generating the equivalent Fmoc protected statin building block **4** (**Scheme 1B**). For convenience, the hydroxymethylcarbonyl and statin variants were prepared



Scheme 1. Synthetic scheme for (A) the preparation of the hydroxymethylcarbonyl Fmoc amino acid **2**, (B) the preparation of the statin Fmoc amino acid **4**, and (C) the preparation of side chain lipidated cysteine Fmoc amino acids **8a** and **8b**.

as their racemates (effectively enabling the simultaneous preparation of two diastereomers of the target peptidomimetic). Synthesis of the lipidated cysteine building blocks commenced from the commercially available Fmoc-L-Cys(Trt)-OH **5** (**Scheme 1C**). Treatment with allyl bromide in the presence of base yielded the desired allyl ester **6** in quantitative yield. Next, selective deprotection of the side chain trityl protecting group, and subsequent alkylation in a biphasic system, generated the octyl lipidated cysteine **7a** and the benzylated cysteine **7b** in good yields. Finally, treatment with palladium tetrakis in the presence of *N*-methylaniline, gave the desired lipidated cysteine Fmoc amino acids **8a** and **8b**, ready for use in SPPS.

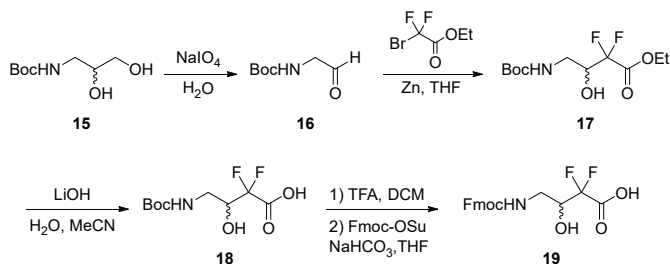
Preparation of the building block containing the reduced amide non-cleavable motif required the synthesis of a dipeptide containing both the reduced amide and cysteine fragments (**Scheme 2**). Fortunately, the previously prepared intermediates **7a** and **7b** were appropriate starting points for this synthesis. Treatment of cysteine derivatives **7a** and **7b** with diethylamine smoothly mediated Fmoc deprotection, yielding the corresponding primary amines **9a** and **9b** respectively. In parallel, Fmoc-glycinol **10** was oxidised to its corresponding aldehyde **11** through the use of Dess–Martin periodinane (DMP). With aldehyde **11** and amines **9a** and **9b** in hand, reductive amination was performed with sodium cyanoborohydride and a catalytic amount of acetic acid in methanol, to generate the desired reduced amide products **12a** and **12b** in modest yields. Next, these secondary amines were Boc protected with Boc anhydride and DIPEA. Finally, treatment with palladium tetrakis yielded the reduced amide containing protected building blocks **14a** and **14b**, ready for incorporation into their respective peptidomimetics.



Scheme 2. Synthetic scheme for the preparation of reduced amide non-cleavable motifs **14a** and **14b**.

The final building block needed for this study was that containing the difluoroketone moiety. Due to the electron-withdrawing properties of the two fluorine atoms in the difluoroketone structure, the partial positive charge in the adjacent ketone carbonyl is enhanced. In the presence of water this results in the formation of a stabilised *gem*-diol that mimics the transition state of aspartyl proteases.²⁸

The synthesis of the difluoroketone containing building block commenced with the synthesis of Boc-glycinal **16**. Initially, this intermediate was formed from Boc-glycinol using DMP. Though effective, the poor atom-economy and need for chromatographic purification led us to instead prepare aldehyde **16** from the Boc protected vicinal diol **15** (**Scheme 3**). Treatment with sodium periodate mediated the oxidative cleavage of the 1,2 carbon-carbon bond yielding Boc-glycinal **16** and formaldehyde. Following simple extraction of the reaction mixture with MTBE, **16** was obtained in high purity and yield. Aldehyde **16** was then submitted to the Reformatsky reaction protocol using ethyl bromodifluoroacetate and metallic zinc powder in refluxing THF to furnish alcohol **17** as a mixture of enantiomers.^{29,30} Ethyl ester **17** was next saponified with 0.25 M lithium hydroxide solution to provide the corresponding free carboxylic acid **18**. Finally, replacement of the amino Boc protecting group with Fmoc was achieved by first treating the pseudo dipeptide **18** with TFA in DCM before reprotection with Fmoc-OSu and sodium bicarbonate. This yielded the desired Fmoc difluoroalcohol carboxylic acid **19**.



Scheme 3. Synthetic scheme for the preparation of the difluoro alcohol non-cleavable motifs **19**.

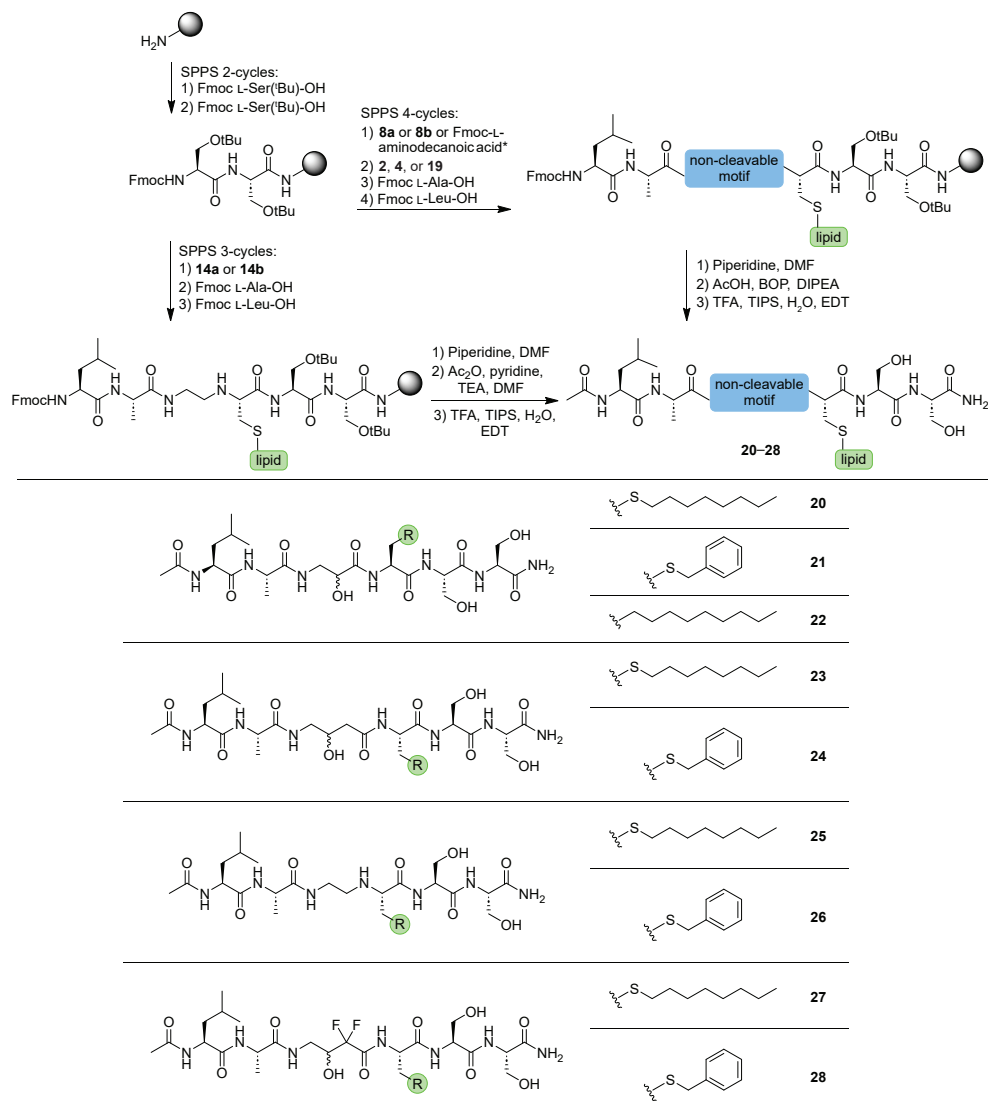
Previous literature solution-phase syntheses of difluoroketone containing peptidomimetics have first formed the difluoroalcohol core, followed by elaboration of the peptide structure, before finally oxidising the difluoroalcohol to its corresponding difluoroketone with either IBX or DMP.^{28,30} Due to concerns over the reactivity of the difluoroketone moiety during peptide synthesis, we decided to follow this literature approach by directly incorporating of the difluoroalcohol pseudodipeptide **19** into the peptide and, following completed synthesis of the peptidomimetic, attempting on-resin oxidation of the difluoroalcohol motif to its

corresponding difluoroketone.³¹ Although there are no literature examples of on-resin oxidation of difluoroalcohols, peptides containing an internal α -hydroxyamide moiety have been successfully oxidised on-resin to α -ketoamides.³¹

With the synthesis of the requisite cysteines and non-cleavable motifs completed, our attention turned to incorporating these building blocks into the peptidomimetics designed using SPPS. Commencing from Rink Amide resin, loaded with *tert*-butyl protected serine, the peptides were assembled using standard Fmoc-SPPS techniques (**Scheme 4**). Following the incorporation of a second serine residue, the peptides were differentiated. Three peptidomimetics were prepared from the hydroxymethylcarbonyl building block **2**. These incorporated the lipidated cysteine building blocks **8a** or **8b**. In addition, a third variant containing an L-aminodecanoic acid residue, in place of a cysteine, was prepared. L-aminodecanoic acid possesses an all carbon side chain of equivalent length to **8a**. This was done to allow for assessment of the thioether's impact on LspA binding affinity. For the statin-, and difluoroalcohol-containing peptidomimetics, either of the lipidated cysteine building blocks **8a** or **8b** were first incorporated, followed by their respective non-cleavable motif **4** or **19**. Considering that the reduced amide containing motifs **14a** and **14b** already contained both the lipidated cysteine and reduced amide motifs within the same building block, only a single SPPS cycle was required.

Next, the remaining L-Ala and L-Leu residues were coupled to all peptides over the course of two additional SPPS cycles. Following a final Fmoc deprotection, the reduced amide containing peptides were then capped with acetic anhydride, pyridine and triethylamine in DMF. Due to the presence of an unprotected hydroxy group in the HMC, statin, and DFA peptides, these were instead capped by coupling acetic acid to their N-termini with the use of BOP and DIPEA.

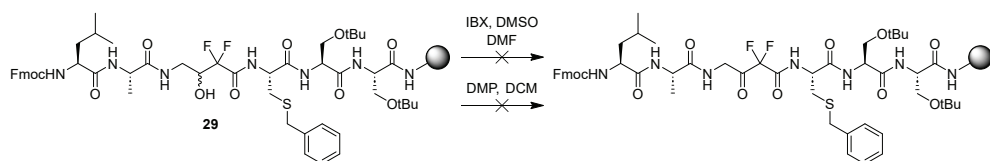
In the case of difluoroalcohol containing peptidomimetics, it was at this stage that an attempt at on-resin oxidation to the corresponding difluoroketone was conducted. An initial attempt at on-resin oxidation of the difluoroalcohol moiety with DMP in DCM, based on a literature solution-phase procedure, did not result in product formation (**Scheme 5**).^{28,30} An attempt using IBX in DMF and DMSO (1:1, *v/v*), following a different literature procedure that utilised on-resin oxidation in the preparation of α -ketoamides, also proved unsuccessful with no conversion observed.³¹ Given its apparent lack of reactivity, the Fmoc-difluoroalcohol amino acid building block **19** was also treated with IBX in DMSO at elevated temperature. The reaction was followed by TLC and LC-MS, and despite overnight heating at 70 °C, no conversion to either the difluoroketone nor its hydrated *gem*-diol form was observed. The lack of reactivity



Scheme 4. Synthesis of peptidomimetic hexamers using solid-phase peptide synthesis and the structures of all peptidomimetics prepared in this study. Commencing from Rink Amide resin loaded with L-Ser successive cycles of SPPS produce the completed protected peptides. Next, the N-termini are capped as acetamides before global deprotection furnishes the completed peptidomimetics. *Fmoc-L-aminodecanoic acid used only in combination with **2** for the preparation of peptidomimetic **22**.

observed for the difluoroalcohol moiety was unexpected considering the successful literature reports of oxidation of similar molecules. A key difference in the literature examples is the presence of a γ -methyl group adjacent to the difluoroalcohol moiety, whereas **19**, derived from glycine, contains two γ -protons in this position. We hypothesise that the absence of this methyl group in the structure of **19** impacted the electronics of the adjacent hydroxyl group,

resulting in attenuated reactivity under oxidising conditions. Additional attempts to oxidise **29** under harsher conditions were ruled out due to concerns about oxidation of the thioether moiety in the adjacent cysteine residue. Nonetheless, considering the high degree of chemical similarity between the hydrated *gem*-diol form of a difluoroketone and a difluoroalcohol, the decision was taken to deprotect peptide **29** at this stage and carry on by testing its activity against LspA together with the other peptidomimetics.



Scheme 5. Unsuccessful oxidation of the difluoroalcohol moiety of **29** to its corresponding difluoroketone.

For the final resin cleavage and deprotection step, all peptides were treated with an acidic cocktail, supplemented with EDT to suppress oxidation of the thioether moiety. This afforded the crude peptidomimetics **20–28**, which were subsequently purified using RP-HPLC. Where possible, diastereomers were separated at this stage and correspondingly labelled **a/b** (e.g. **20a** and **20b**) and tested separately. Diastereomers that were unable to be separated were tested as a mixture.

Activity assays

To assess the ability of peptidomimetics **20–28** to inhibit LspA, they were tested using an in-house FRET assay based on previously published studies using a similar method for quantifying LspA activity.^{12,32} In this assay, an LspA substrate is equipped with a FRET pair (**Fig. S1**). When this FRET substrate is incubated with LspA and the mixture followed over time, the intensity of fluorescence increases linearly, from which the initial velocity can be determined. In the presence of an inhibitor, the rate of increase of fluorescence is decreased, allowing for the inhibition to be quantified. The peptidomimetics **20–28**, and the non-specific aspartyl protease inhibitor pepstatin,³³ were each tested in triplicate at a single concentration of 500 μ M. This was normalised against the inhibition of 500 nM globomycin (**Fig. 5A**). This revealed that the hydroxymethylcarbonyl (HMC) containing peptidomimetics **20a** and **20b** offered the most potent inhibition. The >100% result for **20a** was presumably the consequence of the compound interfering with the fluorescence readout, causing a negative initial velocity and a high initial fluorescence signal. Despite this outlier, the HMC-octyl combination in compounds **20a** and **20b** proved to be the most successful inhibitors of LspA. Interestingly, the replacement of the octyl side chain with benzyl in peptide **21** led to almost complete loss

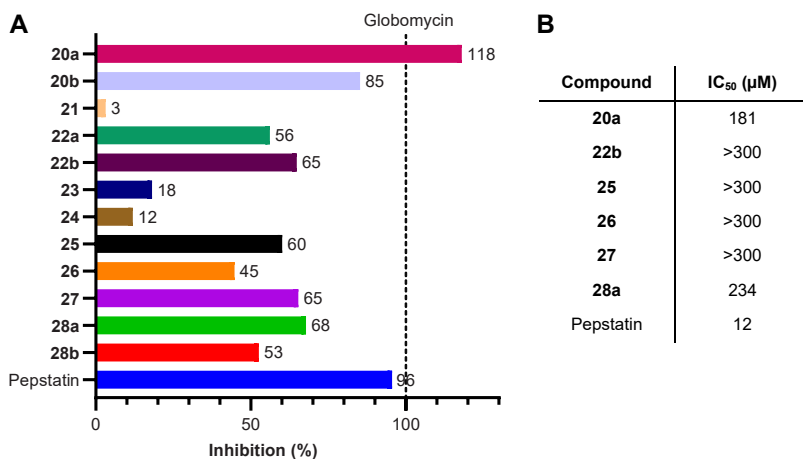


Figure 5. (A) Percentage inhibition of LspA at a fixed concentration of 500 μM. Results are normalised against the inhibition of LspA in the presence of 500 nM of globomycin. **(B)** Quantified half maximal inhibitory concentrations (IC₅₀) values for the most active peptidomimetics against LspA.

of inhibition. This trend also held true for the other peptides, with the peptides containing a benzylated cysteine side chain performing worse than their octyl counterparts. The statin containing peptidomimetics **23** and **24** were the least effective inhibitors. Considering that the statins vary from the hydroxymethylcarbonyl inhibitors by only a single methylene group, this illustrates the finely-tuned spacing required for active site recognition. Interestingly, compounds **22a** and **22b**, those bearing the C₁₀ lipid in place of the thioether lipid, led to only a small loss of activity relative to compounds **20a** and **20b**, demonstrating the feasibility of removing this thioether moiety in the design of future peptidomimetics. The peptides containing the reduced amide (**25** and **26**) and the difluoroalcohol motifs (**27** and **28**) possessed comparable inhibitory activity, slightly attenuated relative to compounds **20a** and **20b**.

Based on the results of this initial inhibition study, the half maximal inhibitory concentrations (IC₅₀) values of the most active compounds were also assessed (**Fig. 5B**). Of the peptidomimetics prepared in this study, **20a** gave the lowest IC₅₀ value of 181 μM, this was however an order of magnitude higher than the non-specific aspartyl protease inhibitor pepstatin.

The antibacterial activities of the prepared peptidomimetics **20–28** were then assessed against a panel of Gram-negative bacteria. Minimum inhibitory concentration (MIC) values were determined using standard broth dilution assays and compared with the MICs measured for polymyxin B (PMB). Unfortunately, even at our highest test concentration of 64 μg mL⁻¹, there was no visible impact on bacterial growth (**Table S1**). We hypothesised that the observed lack

of antibacterial activity may be a consequence of the peptidomimetics inability to pass the outer membrane of these bacterial strains. Polymyxin B nonapeptide (PMBN) is a truncated form of polymyxin B that possesses the ability to permeabilise the outer membrane of bacteria whilst lacking the bactericidal activity of PMB.³⁴ It was recently reported that the addition of PMBN significantly enhances the antibacterial activity of globomycin.¹² Based on these findings, we repeated the MIC experiments with the addition of PMBN ($8\text{ }\mu\text{g mL}^{-1}$) to the assay media. However, despite the addition of PMBN, all of the test compounds remained inactive as antibacterials at the highest test concentration of $64\text{ }\mu\text{g mL}^{-1}$. While this may still be the result of poor cell permeability, we cannot exclude the possibility that the compound simply lack sufficient affinity for LspA to possess antibacterial activity at these concentrations.

Conclusions

This chapter focussed on utilising a rational design approach towards the preparation of the first peptidomimetic inhibitors of LspA. Four classes of non-cleavable motifs were incorporated into short peptides based on the preference LspA substrate sequence and their activity against LspA was measured. Based on initial biological screening, it can be concluded that the majority of the peptidomimetics prepared possess the ability to inhibit LspA, with compound **20a** offering the highest potency. These compounds are however, at best, high- μM inhibitors of LspA. Furthermore, none of the prepared compounds possess antibacterial activity against live bacteria at a concentration of $64\text{ }\mu\text{g mL}^{-1}$, even in the presence of an outer membrane permeabiliser. Further investigations should focus on increasing the binding affinity of the inhibitors for LspA and improving their cell permeability.

The results presented in this chapter give insight into the use of different non-cleavable motifs and lipids incorporated into peptidomimetics inspired by the consensus sequence of LspA. These findings serve as a stepping stone in the development of this novel class of antibacterial compounds. Similar to the development of the clinically used HIV protease inhibitors, these peptidomimetics can hopefully also be iteratively improved in order to generate, more drug-like and highly specific inhibitors of LspA as a new class of antibacterial drugs.

Experimental Procedures

All reagents employed were of American Chemical Society (ACS) grade or higher and were used without further purification unless otherwise stated. LC-MS- and HPLC-grade acetonitrile, peptide grade *N,N*-dimethylformamide (DMF) and dichloromethane (DCM) for peptide synthesis were purchased from Biosolve Chimie SARL and VWR, respectively. Buffers and salts were purchased from Carl Roth GmbH (Karlsruhe, Germany) and VWR International (Leuven, Belgium).

Unless otherwise stated, ^1H NMR and ^{13}C NMR spectra were recorded on a Bruker AV-400 spectrometer. The chemical shifts are noted as δ -values in parts per million (ppm) relative to the signal of CDCl_3 for ^1H NMR ($\delta = 7.26$ ppm) and ^{13}C NMR ($\delta = 77.16$ ppm). Coupling constants (*J*) are given in Hz.

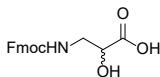
HPLC analyses were performed on a Shimadzu Prominence-i LC-2030 system with a Dr. Maisch ReproSil Gold 120 C18 column (4.6×250 mm, $10\ \mu\text{m}$) at $30\ ^\circ\text{C}$ and equipped with a UV detector monitoring at 214 and 254 nm. The following solvent system, at a flow rate of 1 mL/min, was used: solvent A (0.1 % TFA in water/acetonitrile 95:5); solvent B (0.1 % TFA in water/acetonitrile 5:95). Gradient elution was as follows: 100:0 (A/B) for 2 min, 100:0 to 0:100 (A/B) over 23 min, 0:100 (A/B) for 1 min, then reversion back to 100:0 (A/B) over 1 min, 100:5 (A/B) for 4 min.

LC-MS analysis were performed on a Shimadzu LC-20AD system with a Shimadzu Shim-Pack GISS-HP C18 column (3.0×150 mm, $3\ \mu\text{m}$) at $30\ ^\circ\text{C}$ and equipped with a UV detector. As solvent system, at a flow rate of 0.5 mL/min, solvent A (0.1% formic acid in water) and solvent B (acetonitrile) was used. Gradient elution was as follows: 95:5 A/B for 2 min, 95:5 to 0:100 A/B over 13 min, 0:100 A/B for 2 min, then reversion back to 95:5 A/B over 1 min, 95:5 A/B for 3 min. This system was connected to a Shimadzu 8040 triple quadrupole mass spectrometer (ESI ionisation).

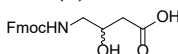
High resolution mass spectra (HRMS) were recorded on a Shimadzu Nexera X2 UHPLC system with a Waters Acquity HSS C18 column (2.1×100 mm, $1.8\ \mu\text{m}$) at $30\ ^\circ\text{C}$ and equipped with a diode array detector. The following solvent system, at a flow rate of 0.5 mL/min, was used: solvent A, 0.1 % formic acid in water; solvent B, 0.1 % formic acid in acetonitrile. Gradient elution was as follows: 95:5 (A/B) for 1 min, 95:5 to 15:85 (A/B) over 6 min, 15:85 to 0:100 (A/B) over 1 min, 0:100 (A/B) for 3 min, then reversion back to 95:5 (A/B) for 3 min. This system was connected to a Shimadzu 9030 QTOF mass spectrometer (ESI ionisation) calibrated internally with Agilent's API-TOF reference mass solution kit (5.0 mM purine, 100.0 mM ammonium trifluoroacetate and 2.5 mM hexakis(1*H*,1*H*,3*H*-tetrafluoropropoxy)phosphazine) diluted to achieve a mass count of 10,000.

Chemical Synthesis

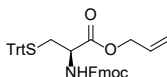
3-(Fmoc)amino-2-hydroxypropanoic acid (2)



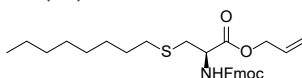
Isoserine (**1**) (2.00 g, 19 mmol) was dissolved in a mixture of aqueous NaHCO_3 (10% w/w, 76 mL) and THF (19 mL). A solution of FmocOSu (6.41 g, 19 mmol) in THF (57 mL) was added dropwise. The reaction was stirred for three days until complete (TLC: 20% MeOH in DCM). The volatiles were removed under reduced pressure and the remaining solution was treated with aqueous HCl (4 % v/v, ca. 140 mL) until pH 2 was reached. The aqueous layer was extracted with EtOAc, washed with brine, dried over Na_2SO_4 and concentrated. Trituration with Et_2O gave the title compound **2** (5.27 g, 85%). ^1H NMR (400 MHz, DMSO- d_6) δ 7.88 (d, $J = 7.5$ Hz, 2H), 7.71 (d, $J = 7.4$ Hz, 2H), 7.45 – 7.36 (m, 3H), 7.33 (t, $J = 7.3$ Hz, 2H), 4.30 – 4.24 (m, 2H), 4.23 – 4.17 (m, 1H), 4.04 (dd, $J = 7.0, 4.8$ Hz, 1H), 3.32 (dt, $J = 13.4, 5.2$ Hz, 1H), 3.16 (dt, $J = 13.5, 6.6$ Hz, 1H). ^{13}C NMR (101 MHz, DMSO- d_6) δ 174.5, 156.7, 144.3, 141.2, 128.1, 127.6, 125.7, 120.6, 69.8, 66.0, 47.1, 44.7. HRMS (ESI) m/z : $[\text{M}+\text{H}]^+$ calculated $\text{C}_{18}\text{H}_{17}\text{NO}_3$: 328.1180, found: 328.1182.

4-(Fmoc)amino-3-hydroxybutanoic acid (4)

4-Amino-3-hydroxybutyric acid (1.79 g, 15 mmol) was dissolved in a mixture of aqueous NaHCO_3 (10% w/w, 60 mL) and THF (15 mL). A solution of FmocOSu (5.06 g, 15 mmol) in THF (45 mL) was added slowly. The reaction stirred for three days until complete (TLC: 15% MeOH in DCM). The volatiles were removed under reduced pressure and the remaining solution was treated with aqueous HCl (4 % v/v, ca. 140 mL) until pH 2 was reached. The aqueous layer was extracted with EtOAc, washed with brine, dried over Na_2SO_4 and concentrated to afford the title compound **4** (4.07 g, 79%). ^1H NMR (400 MHz, $\text{DMSO}-d_6$) δ 7.90 (d, J = 7.5 Hz, 2H), 7.72 (d, J = 7.4 Hz, 2H), 7.42 (t, J = 7.4 Hz, 2H), 7.34 (t, J = 7.0 Hz, 3H), 4.30 (d, J = 7.1 Hz, 2H), 4.22 (t, J = 6.9 Hz, 1H), 3.96 – 3.84 (m, 1H), 3.10 – 2.94 (m, 2H), 2.39 (dd, J = 15.3, 3.9 Hz, 1H), 2.16 (dd, J = 15.3, 8.8 Hz, 1H). ^{13}C NMR (101 MHz, $\text{DMSO}-d_6$) δ 172.9, 156.3, 143.9, 140.8, 127.7, 127.1, 125.3, 120.2, 66.7, 65.4, 46.8, 46.4, 40.1. HRMS (ESI) m/z : $[\text{M}+\text{H}]^+$ calculated $\text{C}_{19}\text{H}_{19}\text{NO}_5$: 342.1336, found: 342.1338.

allyl N-Fmoc-S-trityl-L-cysteinate (6)

N-Fmoc-S-trityl-L-cysteine (**5**) (30.0 g, 51.2 mmol) was dissolved in dry DMF (340 mL). Caesium carbonate (8.34 g, 26.6 mmol, 0.50 eq.) was added, followed by the dropwise addition of allyl bromide (4.34 mL, 51.2 mmol, 1.0 eq.) and the mixture was stirred overnight. After complete conversion, $\approx 70\%$ of the solvent was removed *in vacuo*. The remaining mixture was diluted with EtOAc and washed 4 times with water. The organic layer was then washed with brine, dried over Na_2SO_4 , filtered and concentrated *in vacuo*. The crude product was purified by silica gel column chromatography eluting with 10–20% EtOAc in petroleum ether yielding Allyl N-Fmoc-S-trityl-L-cysteinate **6** as a white solid (32.0 g, 51.1 mmol, quant.). ^1H NMR (400 MHz, CDCl_3) δ 7.78 (dd, J = 7.5, 3.7 Hz, 2H), 7.61 (dd, J = 7.3, 2.6 Hz, 2H), 7.43 – 7.38 (m, 8H), 7.30 (dd, J = 12.9, 7.2 Hz, 7H), 7.24 – 7.19 (m, 3H), 5.88 (ddd, J = 22.8, 10.9, 5.7 Hz, 1H), 5.37 – 5.22 (m, 3H), 4.69 – 4.55 (m, 2H), 4.43 – 4.31 (m, 3H), 4.24 (t, J = 7.1 Hz, 1H), 2.67 (qd, J = 12.4, 5.5 Hz, 2H). ^{13}C NMR (101 MHz, CDCl_3) δ 170.3 (C), 155.7 (C), 144.4 (C), 144.0 (C), 143.8 (C), 141.4 (C), 131.5 (CH), 129.6 (CH), 128.2 (CH), 127.9 (CH), 127.2 (CH), 127.0 (CH), 125.3 (CH), 120.1 (CH), 119.0 (CH_2), 67.3 (CH_2), 66.4 (CH_2), 53.1 (CH), 47.2 (CH), 34.2 (CH_2). HRMS (ESI) m/z : $[\text{M}+\text{Na}]^+$ calculated $\text{C}_{40}\text{H}_{35}\text{NO}_4\text{Na}$: 648.2185, found: 648.2178.

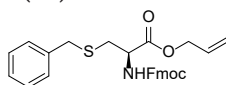
allyl N-Fmoc-S-octyl-L-cysteinate (7a)

Allyl N-Fmoc-S-trityl-L-cysteinate (**6**) (15.6 g, 25.0 mmol) was dissolved in DCM (250 mL) and cooled to 0 °C. TIPS (10.2 mL, 50.0 mmol, 2.0 eq.) and TFA (19.1 mL, 250 mmol, 10 eq.) were then added dropwise. The mixture was allowed to warm to r.t. and was stirred for 1 hour. Water (250 mL) was added slowly followed by NaHCO_3 (21.0 g, 250 mmol) to quench excess acid. The layers were separated and the organic layer was washed with brine, dried over Na_2SO_4 , filtered and concentrated *in vacuo*. Crude allyl Fmoc-L-cysteinate was obtained as a white solid (23.7 g, 61.8 mmol, quant.) and was used immediately without further purification.

Allyl Fmoc-L-cysteinate (9.47 g, 24.7 mmol) was dissolved in EtOAc (165 mL) and octyl bromide (4.69 mL, 27.2 mmol, 1.1 eq.) was added dropwise. To the mixture, a solution of tetrabutyl ammoniumbromide (31.9 g, 98.8 mmol, 4.0 eq.) in sat. aq. NaHCO_3 (200 mL) was added before stirring vigorously overnight. The reaction mixture was then diluted with EtOAc and water until transparent.

The layers were separated and the organic layer was washed with brine, dried over Na_2SO_4 , filtered and concentrated *in vacuo*. The crude product was purified by silica gel column chromatography eluting with 20–50% EtOAc in petroleum ether yielding Allyl *N*-Fmoc-S-octyl-L-cysteinate **7a** as a colourless oil (7.61 g, 15.4 mmol, 61%). ^1H NMR (400 MHz, CDCl_3) δ 7.77 (d, J = 7.5 Hz, 2H), 7.65 – 7.58 (m, 2H), 7.41 (td, J = 7.5, 1.1 Hz, 2H), 7.32 (td, J = 7.5, 1.2 Hz, 2H), 5.93 (ddt, J = 16.4, 10.4, 5.8 Hz, 1H), 5.68 (d, J = 8.0 Hz, 1H), 5.37 (dq, J = 17.3, 1.4 Hz, 1H), 5.28 (dq, J = 10.4, 1.3 Hz, 1H), 4.68 (dt, J = 6.0, 1.5 Hz, 2H), 4.66 – 4.60 (m, 1H), 4.40 (d, J = 7.6 Hz, 2H), 4.25 (t, J = 7.2 Hz, 1H), 3.02 (dd, J = 5.1, 1.8 Hz, 2H), 2.53 (t, J = 7.4 Hz, 2H), 1.62 – 1.50 (m, 2H), 1.39 – 1.21 (m, 10H), 0.87 (t, J = 7.0 Hz, 3H). ^{13}C NMR (101 MHz, CDCl_3) δ 170.7 (C), 155.9 (C), 144.0 (C), 143.9 (C), 141.4 (C), 131.5 (CH), 127.9 (CH), 127.2 (CH), 125.3 (CH), 120.1 (CH), 119.3 (CH_2), 67.4 (CH_2), 66.5 (CH_2), 53.8 (CH), 47.2 (CH), 34.6 (CH_2), 33.0 (CH_2), 31.9 (CH_2), 29.7 (CH_2), 29.3 (CH_2), 28.9 (CH_2), 22.78 (CH_2), 14.2 (CH_3). HRMS (ESI) m/z : $[\text{M}+\text{H}]^+$ calculated $\text{C}_{29}\text{H}_{37}\text{NO}_4$: 496.2516, found: 496.2519.

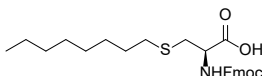
allyl *N*-Fmoc-S-benzyl-L-cysteinate (**7b**)



Allyl *N*-Fmoc-S-trityl-L-cysteinate (**6**) (15.6 g, 25.0 mmol) was dissolved in DCM (250 mL) and cooled to 0 °C. TIPS (10.2 mL, 50.0 mmol, 2.0 eq.) and TFA (19.1 mL, 250 mmol, 10 eq.) were then added dropwise. The mixture was allowed to warm to r.t. and was stirred for 1 h. Water (250 mL) was added slowly, followed by NaHCO_3 (21.0 g, 250 mmol) to quench excess acid. The layers were separated and the organic layer was washed with brine, dried over Na_2SO_4 , filtered and concentrated *in vacuo*. Crude allyl Fmoc-L-cysteinate was obtained as a white solid (23.7 g, 61.8 mmol, quant.) and was used immediately without further purification.

Allyl Fmoc-L-cysteinate (9.59 g, 25.0 mmol) was dissolved EtOAc (166 mL) and benzyl bromide (3.23 mL, 27.5 mmol, 1.1 eq.) was added dropwise. To the mixture, a solution of tetrabutyl ammoniumbromide (32.2 g, 100 mmol, 4.0 eq.) in sat. aq. NaHCO_3 (200 mL) was added before stirring vigorously overnight. The reaction mixture was diluted with EtOAc and water until transparent. The layers were separated and the organic layer was washed with brine, dried over Na_2SO_4 , filtered and concentrated *in vacuo*. The crude product was purified by silica gel column chromatography eluting with 0–20% EtOAc in petroleum ether yielding Allyl *N*-Fmoc-S-benzyl-L-cysteinate **7b** as a white solid (9.45 g, 20.0 mmol, 80%). ^1H NMR (400 MHz, CDCl_3) δ 7.81 – 7.75 (m, 2H), 7.63 (dd, J = 7.5, 3.8 Hz, 2H), 7.45 – 7.38 (m, 2H), 7.36 – 7.28 (m, 6H), 7.28 – 7.24 (m, 1H), 5.98 – 5.85 (m, 1H), 5.62 (d, J = 8.1 Hz, 1H), 5.35 (dq, J = 17.2, 1.5 Hz, 1H), 5.28 (dq, J = 10.5, 1.3 Hz, 1H), 4.72 – 4.60 (m, 3H), 4.43 (d, J = 7.2 Hz, 2H), 4.26 (t, J = 7.1 Hz, 1H), 3.73 (s, 2H), 2.92 (qd, J = 13.9, 5.4 Hz, 2H). ^{13}C NMR (101 MHz, CDCl_3) δ 170.6 (C), 155.8 (C), 143.9 (C), 143.8 (C), 141.4 (C), 137.6 (C), 131.4 (C), 129.1 (CH), 128.7 (CH), 127.8 (CH), 127.4 (CH), 127.2 (CH), 125.2 (CH), 120.1 (CH), 119.2 (CH_2), 67.3 (CH_2), 66.4 (CH_2), 53.7 (CH), 47.2 (CH), 36.8 (CH_2), 33.7 (CH_2). HRMS (ESI) m/z : $[\text{M}+\text{H}]^+$ calculated $\text{C}_{28}\text{H}_{27}\text{NO}_4\text{S}$: 474.1734, found: 474.1737.

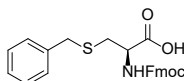
N-Fmoc-S-octyl-L-cysteine (**8a**)



Allyl *N*-Fmoc-S-octyl-L-cysteinate (**7a**) (2.48 g, 5.00 mmol) was dissolved in dry THF (50 mL). $\text{Pd}(\text{PPh}_3)_4$ (173 mg, 0.150 mmol, cat.) and *N*-methylaniline (1.62 mL, 15.0 mmol, 3.0 eq.) were added and the mixture was stirred for 2 h while protected from light. The mixture was then diluted with EtOAc and washed with water. The organic layer was then washed with brine, dried over Na_2SO_4 , filtered and concentrated *in vacuo*. The crude product was purified by silica gel column chromatography eluting with 0–5% MeOH in DCM (with 1% AcOH) yielding *N*-Fmoc-S-octyl-L-cysteine **8a** as a white solid

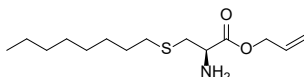
(1.81 g, 3.47 mmol, 69%). ^1H NMR (400 MHz, CDCl_3) δ 9.12 (br, 1H), 7.76 (d, $J = 7.5$ Hz, 2H), 7.62 (dd, $J = 7.6, 2.9$ Hz, 2H), 7.40 (t, $J = 7.5$ Hz, 2H), 7.36 – 7.27 (m, 2H), 5.79 (d, $J = 7.8$ Hz, 1H), 4.61 (dt, $J = 7.9, 5.3$ Hz, 1H), 4.47 – 4.36 (m, 2H), 4.24 (t, $J = 7.2$ Hz, 1H), 3.12 – 2.96 (m, 2H), 2.55 (t, $J = 7.0$ Hz, 2H), 1.56 (p, $J = 7.2$ Hz, 2H), 1.44 – 1.17 (m, 10H), 0.88 (t, $J = 6.8$ Hz, 3H). ^{13}C NMR (101 MHz, CDCl_3) δ 175.4 (C), 156.2 (C), 143.9 (C), 141.4 (C), 127.9 (CH), 127.2 (CH), 125.2 (CH), 120.1 (CH), 67.45 (CH_2), 53.9 (CH), 47.2 (CH), 34.3 (CH_2), 33.0 (CH_2), 31.9 (CH_2), 29.6 (CH_2), 29.3 (CH_2), 28.9 (CH_2), 22.8 (CH_2), 14.2 (CH_3). HRMS (ESI) m/z : $[\text{M}+\text{H}]^+$ calculated $\text{C}_{26}\text{H}_{33}\text{NO}_4\text{S}$: 456.2203, found: 456.2202.

N-Fmoc-S-benzyl-L-cysteine (8b)



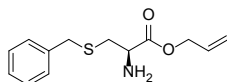
Allyl *N*-Fmoc-S-benzyl-L-cysteinate (**7b**) (2.37 g, 5.00 mmol) was dissolved in dry THF (50 mL). $\text{Pd}(\text{PPh}_3)_4$ (173 mg, 0.150 mmol, cat.) and *N*-methylaniline (1.62 mL, 15.0 mmol, 3.0 eq.) were added and the mixture was stirred for 2 h while protected from light. The mixture was then diluted with EtOAc and washed with water. The organic layer was then washed with brine, dried over Na_2SO_4 , filtered and concentrated *in vacuo*. The crude product was purified by silica gel column chromatography eluting with 0–5% MeOH in DCM (with 1% AcOH) yielding *N*-Fmoc-S-benzyl-L-cysteine **8b** as a white solid (1.41 g, 3.26 mmol, 65%). ^1H NMR (400 MHz, CDCl_3) δ 7.72 (dd, $J = 7.6, 3.0$ Hz, 2H), 7.56 (t, $J = 7.8$ Hz, 2H), 7.35 (td, $J = 7.5, 4.3$ Hz, 2H), 7.28 – 7.12 (m, 7H), 5.79 (s, 1H), 4.49 (s, 1H), 4.41 – 4.23 (m, 2H), 4.17 (t, $J = 7.2$ Hz, 1H), 3.67 (s, 2H), 2.97 – 2.79 (m, 2H). ^{13}C NMR (101 MHz, CDCl_3) δ 156.3 (C), 144.0 (C), 143.8 (C), 141.4 (C), 137.8 (C), 129.1 (CH), 128.7 (CH), 127.8 (CH), 127.3 (CH), 127.2 (CH), 125.3 (CH), 120.1 (CH), 67.4 (CH_2), 54.1 (CH), 47.2 (CH), 36.8 (CH_2), 33.7 (CH_2). HRMS (ESI) m/z : $[\text{M}+\text{H}]^+$ calculated $\text{C}_{25}\text{H}_{23}\text{NO}_4\text{S}$: 434.1421, found: 434.1422.

allyl S-octyl-L-cysteinate (9a)



Allyl *N*-Fmoc-S-octyl-L-cysteinate (**7a**) (7.44 g, 15.0 mmol) was dissolved in MeCN (75.0 mL). Diethylamine (62.0 mL, 600 mmol, 40 eq.) was added and the mixture was stirred for 2 hours before concentrating *in vacuo*. The crude product was purified by silica gel column chromatography eluting with 20–50% EtOAc in petroleum ether (with 1% TEA) yielding Allyl S-octyl-L-cysteinate **9a** as a transparent oil (3.23 g, 11.8 mmol, 79%). ^1H NMR (400 MHz, CDCl_3) δ 5.86 (ddt, $J = 17.2, 10.4, 5.8$ Hz, 1H), 5.28 (dq, $J = 17.2, 1.5$ Hz, 1H), 5.20 (dq, $J = 10.4, 1.3$ Hz, 1H), 4.57 (dt, $J = 5.8, 1.4$ Hz, 2H), 3.60 (dd, $J = 7.3, 4.7$ Hz, 1H), 2.96 – 2.63 (m, 2H), 2.68 (s, 1H), 2.46 (t, $J = 7.6$ Hz, 2H), 1.86 (s, 2H), 1.50 (p, $J = 7.7$ Hz, 2H), 1.35 – 1.11 (m, 10H), 0.86 – 0.77 (m, 3H). ^{13}C NMR (101 MHz, CDCl_3) δ 173.7 (C), 131.8 (C), 118.9 (CH_2), 65.9 (CH_2), 54.2 (CH), 37.1 (CH_2), 32.7 (CH_2), 31.8 (CH_2), 31.0 (CH), 29.7 (CH_2), 29.2 (CH_2), 28.8 (CH_2), 22.7 (CH_2), 14.1 (CH_3). HRMS (ESI) m/z : $[\text{M}+\text{H}]^+$ calculated $\text{C}_{14}\text{H}_{27}\text{NO}_2\text{S}$: 274.1835, found: 274.1836.

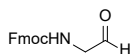
allyl S-benzyl-L-cysteinate (9b)



Allyl *N*-Fmoc-S-benzyl-L-cysteinate (**7b**) (1.00 g, 2.11 mmol) was dissolved in MeCN (10.0 mL). Diethylamine (8.73 mL, 84.4 mmol, 40 eq.) was added and the mixture was stirred for 2 hours before concentrating *in vacuo*. The crude product was purified by silica gel column chromatography eluting with 10–30% EtOAc in petroleum ether (with 2% TEA) yielding Allyl S-benzyl-L-cysteinate **9b** as a

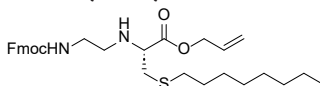
transparent oil (466 mg, 1.84 mmol, 87%). ^1H NMR (400 MHz, CDCl_3) δ 7.32 – 7.27 (m, 4H), 7.25 – 7.19 (m, 1H), 5.88 (ddt, J = 17.2, 10.4, 5.8 Hz, 1H), 5.30 (dq, J = 17.2, 1.5 Hz, 1H), 5.23 (dq, J = 10.5, 1.3 Hz, 1H), 4.60 (dt, J = 5.8, 1.4 Hz, 2H), 3.72 (s, 2H), 3.66 (dd, J = 7.4, 4.7 Hz, 1H), 2.90 – 2.66 (m, 2H). ^{13}C NMR (101 MHz, CDCl_3) δ 173.1 (C), 137.8 (C), 131.5 (CH), 128.9 (CH), 128.5 (CH), 127.1 (CH), 118.7 (CH_2), 65.8 (CH_2), 53.8 (CH), 36.5 (CH_2), 35.9 (CH_2). HRMS (ESI) m/z : $[\text{M}+\text{H}]^+$ calculated $\text{C}_{13}\text{H}_{17}\text{NO}_2\text{S}$: 252.1053, found: 252.1056.

Fmoc-glycinal (**11**)

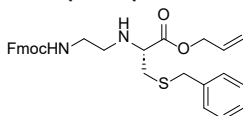


Fmoc-glycinol (**10**) (1.98 g, 7.00 mmol) and Dess–Martin periodinane (DMP) (3.56 mg, 8.40 mmol, 1.2 eq.) were dissolved in DCM (35.0 mL) and cooled to 0 °C. The mixture was stirred for 1.5 hours and allowed to warm to r.t. before stirring overnight. The reaction mixture was diluted with water and washed twice with sat. aq. NaHCO_3 . The combined aqueous layers were extracted with DCM. Next, the combined organic layers were washed with brine, dried over Na_2SO_4 , filtered and concentrated *in vacuo*. The crude product was purified by silica gel column chromatography eluting with 40% EtOAc in petroleum ether yielding the title compound **11** as a white solid (1.69 g, 6.02 mmol, 86%). ^1H NMR (400 MHz, CDCl_3) δ 9.63 (s, 1H), 7.77 (d, J = 7.7 Hz, 3H), 7.60 (d, J = 7.5 Hz, 3H), 7.41 (t, J = 7.2 Hz, 3H), 7.32 (td, J = 7.5, 1.2 Hz, 3H), 5.54 (t, J = 5.2 Hz, 1H), 4.43 (d, J = 7.0 Hz, 3H), 4.23 (t, J = 6.9 Hz, 2H), 4.19 – 4.12 (m, 2H). ^{13}C NMR (101 MHz, CDCl_3) δ 196.7 (CH), 156.4 (C), 143.8 (C), 141.4 (C), 127.9 (CH), 127.2 (CH), 125.1 (CH), 120.1 (CH), 67.3 (CH_2), 51.7 (CH_2), 47.2 (CH). HRMS (ESI) m/z : $[\text{M}+\text{H}]^+$ calculated $\text{C}_{17}\text{H}_{15}\text{NO}_3$: 282.1125, found: 282.1124.

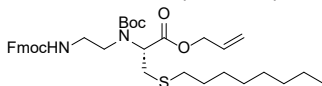
allyl N-(2-((Fmoc)amino)ethyl)-S-octyl-L-cysteinate (**12a**)



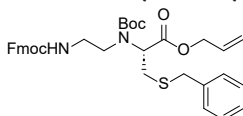
Allyl S-octyl-L-cysteinate (**9a**) (3.06 g, 12.2 mmol) was dissolved in dry methanol (122 mL). Fmoc-glycinal (**11**) (3.25 g, 11.6 mmol, 0.95 eq.) was added together with 3 Å molecular sieves (~50). The mixture was cooled to 0 °C and stirred for 3 h at the same temperature. NaBH_3CN (1.15 g, 18.3 mmol, 1.5 eq.) and AcOH (*ca.* 3 drops, cat.) were added and the mixture was stirred at r.t. overnight. The solvent was removed *in vacuo* and the residue was redissolved EtOAc. The mixture was washed with sat. aq. NaHCO_3 . The aqueous layer was then extracted three times with EtOAc. The combined organic layers were washed with brine, dried over Na_2SO_4 , filtered and concentrated *in vacuo*. The crude product was purified by silica gel column chromatography eluting with 20–50% EtOAc in petroleum ether (with 1% TEA) yielding allyl N-(2-((Fmoc)amino)ethyl)-S-octyl-L-cysteinate **12a** as a transparent oil (697 mg, 1.29 mmol, 11%). ^1H NMR (400 MHz, CDCl_3) δ 7.75 (dt, J = 7.6, 1.0 Hz, 2H), 7.61 (d, J = 7.5 Hz, 2H), 7.39 (ddt, J = 8.3, 7.5, 0.8 Hz, 2H), 7.30 (td, J = 7.5, 1.2 Hz, 2H), 5.99 – 5.86 (m, 1H), 5.50 (t, J = 5.6 Hz, 1H), 5.34 (dt, J = 17.2, 1.3 Hz, 1H), 5.26 (dq, J = 10.3, 1.3 Hz, 1H), 4.64 (ddt, J = 5.8, 4.4, 1.4 Hz, 2H), 4.45 – 4.31 (m, 2H), 4.22 (t, J = 7.1 Hz, 1H), 3.46 (dd, J = 7.2, 5.5 Hz, 1H), 3.39 – 3.14 (m, 2H), 3.11 – 2.65 (m, 4H), 2.52 (dd, J = 7.9, 6.9 Hz, 2H), 2.20 – 2.00 (br, 1H), 1.62 – 1.50 (m, 2H), 1.40 – 1.14 (m, 10H), 0.94 – 0.78 (m, 3H). ^{13}C NMR (101 MHz, CDCl_3) δ 173.3 (C), 156.6 (C), 144.1 (C), 141.4 (C), 131.8 (CH), 127.7 (CH), 127.1 (CH), 125.2 (CH), 120.0 (CH), 119.0 (CH_2), 66.8 (CH_2), 65.9 (CH_2), 60.9 (CH), 47.3 (CH_2), 47.2 (CH_2), 40.8 (CH_2), 35.4 (CH_2), 32.9 (CH_2), 31.9 (CH_2), 29.7 (CH_2), 29.3 (CH_2), 28.9 (CH_2), 22.7 (CH_2), 14.9 (CH_3). HRMS (ESI) m/z : $[\text{M}+\text{H}]^+$ calculated $\text{C}_{31}\text{H}_{42}\text{N}_2\text{O}_4\text{S}$: 539.2938, found: 539.2948.

allyl *N*-(2-((Fmoc)amino)ethyl)-*S*-benzyl-L-cysteinate (12b)

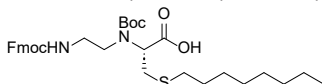
Allyl *S*-benzyl-L-cysteinate (**9b**) (1.62 g, 6.40 mmol) was dissolved in dry methanol (130 mL). Fmoc-glycinal (**11**) (1.71 g, 6.08 mmol, 0.95 eq.) was added together with 3 Å molecular sieves (~20). The mixture was cooled to 0 °C and stirred for 3 hours at the same temperature. NaBH₃CN (602 mg, 9.60 mmol, 1.5 eq.) and AcOH (3 drops, cat.) were added and the mixture was stirred at r.t. overnight. The solvent was removed *in vacuo* and the residue was redissolved in a 50/50 (v/v) mixture of EtOAc and methanol. The mixture was washed with sat. aq. NaHCO₃. The aqueous layer was then extracted three times with EtOAc. The combined organic layers were washed with brine, dried over Na₂SO₄, filtered and concentrated *in vacuo*. The crude product was purified by silica gel column chromatography eluting with 20–50% EtOAc in petroleum ether (with 1% TEA) yielding allyl *N*-(2-((Fmoc)amino)ethyl)-*S*-benzyl-L-cysteinate **12b** as a transparent oil (1.39 g, 2.69 mmol, 44%). ¹H NMR (400 MHz, CDCl₃) δ 7.72 (d, *J* = 7.6 Hz, 2H), 7.57 (d, *J* = 7.5 Hz, 2H), 7.35 (t, *J* = 7.5 Hz, 2H), 7.32 – 7.21 (m, 6H), 7.22 – 7.20 (m, 1H), 5.86 (ddt, *J* = 16.5, 10.5, 5.8 Hz, 1H), 5.40 (t, *J* = 4.5 Hz, 1H), 5.28 (dq, *J* = 17.2, 1.6 Hz, 1H), 5.22 (dq, *J* = 10.5, 1.3 Hz, 1H), 4.58 (dt, *J* = 5.9, 1.4 Hz, 2H), 4.35 (d, *J* = 7.2 Hz, 2H), 4.18 (t, *J* = 7.1 Hz, 1H), 3.69 (s, 2H), 3.34 (t, *J* = 6.5 Hz, 1H), 3.29 – 3.13 (m, 2H), 2.83 – 2.47 (m, 4H). ¹³C NMR (101 MHz, CDCl₃) δ 156.7 (C), 144.1 (C), 141.4 (C), 138.1 (C), 131.7 (CH), 129.1 (CH), 128.7 (CH), 127.8 (CH), 127.3 (CH), 127.1 (CH), 125.3 (CH), 120.1 (CH), 119.1 (CH₂), 66.8 (CH₂), 66.0 (CH₂), 60.6 (CH), 47.4 (CH), 47.2 (CH₂), 40.6 (CH₂), 37.0 (CH₂), 34.5 (CH₂). HRMS (ESI) *m/z*: [M+H]⁺ calculated C₃₀H₃₂N₂O₄S: 517.2156, found: 517.2132.

allyl *N*-(2-((Fmoc)amino)ethyl)-*N*-(*tert*-butoxycarbonyl)-*S*-octyl-L-cysteinate (13a)

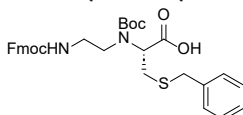
Allyl *N*-(2-((Fmoc)amino)ethyl)-*S*-octyl-L-cysteinate (**12a**) (800 mg, 1.49 mmol) was dissolved in DCM (29.8 mL, 0.050 M). Boc anhydride (648 mg, 2.97 mmol, 2 eq.) and DIPEA (0.779 mL, 4.47 mmol, 3 eq.) were added and the mixture was stirred for 4 days. The reaction mixture was then concentrated *in vacuo*, redissolved in EtOAc and washed with water. The aqueous layer was extracted with EtOAc. The combined organic layers were washed with brine, dried over Na₂SO₄, filtered, and concentrated *in vacuo*. The crude product was purified by silica gel column chromatography eluting with 0–40% EtOAc in petroleum ether yielding allyl *N*-(2-((Fmoc)amino)ethyl)-*N*-(*tert*-butoxycarbonyl)-*S*-octyl-L-cysteinate **13a** as a transparent oil (289 mg, 0.452 mmol, 30%). ¹H NMR (400 MHz, CDCl₃) δ 7.76 (d, *J* = 7.7 Hz, 2H), 7.63 – 7.58 (m, 2H), 7.39 (t, *J* = 7.4 Hz, 2H), 7.34 – 7.28 (m, 2H), 5.86 (ddt, *J* = 16.6, 10.3, 6.0 Hz, 1H), 5.78 (t, *J* = 5.4 Hz, 1H), 5.39 – 5.26 (m, 1H), 5.26 – 5.19 (m, 1H), 4.69 – 4.48 (m, 2H), 4.46 – 4.34 (m, 2H), 4.20 (t, *J* = 6.8 Hz, 1H), 3.96 – 3.61 (m, 1H), 3.49 – 3.32 (m, 2H), 3.29 – 2.98 (m, 4H), 2.51 (td, *J* = 7.3, 2.4 Hz, 2H), 1.61 – 1.49 (m, 2H), 1.42 (s, 9H), 1.38 – 1.18 (m, 10H), 0.91 – 0.83 (m, 3H). ¹³C NMR (101 MHz, CDCl₃) δ 170.4 (C), 144.1 (C), 141.4 (C), 131.3 (CH), 127.8 (CH), 127.1 (CH), 125.2 (CH), 119.8 (CH), 119.5 (CH₂), 66.5 (CH₂), 62.0 (CH), 49.7 (CH), 47.5 (CH₂), 40.4 (CH), 33.0 (CH₂), 31.9 (CH₂), 29.8 (CH₂), 29.3 (CH₂), 29.0 (CH₂), 28.4 ((CH₃)₃), 22.8 (CH₂), 14.2 (CH₃). HRMS (ESI) *m/z*: [M+H]⁺ calculated C₃₆H₅₀N₂O₆S: 639.3463, found: 639.3466.

allyl *N*-(2-((Fmoc)amino)ethyl)-*N*-(*tert*-butoxycarbonyl)-*S*-benzyl-L-cysteinate (13b)


Allyl *N*-(2-((Fmoc)amino)ethyl)-*S*-benzyl-L-cysteinate (**12b**) (300 mg, 0.581 mmol) was dissolved in DCM (11.6 mL). Boc anhydride (190 mg, 0.872 mmol, 1.5 eq.) and DIPEA (121 μ L, 0.697 mmol, 1.2 eq.) were added. The mixture was heated to 40 °C and stirred for 2 days. More Boc anhydride (190 mg, 0.872 mmol) and DIPEA (121 μ L, 0.697 mmol) were added and the mixture was stirred at the same temperature for 3 additional days. The reaction mixture was then concentrated *in vacuo*, redissolved in EtOAc and washed with water. The aqueous layer was extracted with EtOAc. The combined organic layers were washed with brine, dried over Na_2SO_4 , filtered and concentrated *in vacuo*. The crude product was purified by silica gel column chromatography eluting with 20–40% EtOAc in petroleum ether yielding allyl *N*-(2-((Fmoc)amino)ethyl)-*N*-(*tert*-butoxycarbonyl)-*S*-benzyl-L-cysteinate **13b** as a transparent oil (265 mg, 0.430 mmol, 74%). ^1H NMR (400 MHz, CDCl_3) δ 7.76 (dd, J = 7.5, 3.1 Hz, 2H), 7.61 (d, J = 7.4 Hz, 2H), 7.39 (td, J = 7.4, 4.8 Hz, 2H), 7.34 – 7.27 (m, 6H), 7.27 – 7.20 (m, 1H), 5.85 (ddt, J = 16.5, 10.4, 5.9 Hz, 1H), 5.79 – 5.68 (m, 1H), 5.29 (dd, J = 17.1, 1.6 Hz, 1H), 5.22 (dd, J = 10.4, 3.5 Hz, 1H), 4.60 – 4.47 (m, 2H), 4.40 (tt, J = 10.6, 4.7 Hz, 2H), 4.21 (t, J = 6.8 Hz, 1H), 3.77 – 3.69 (m, 3H), 3.44 – 3.21 (m, 2H), 3.18 – 2.93 (m, 4H), 1.50 – 1.34 (m, 9H). ^{13}C NMR (101 MHz, CDCl_3) δ 170.3 (C), 156.5 (C), 155.0 (C), 144.0 (C), 141.3 (C), 138.2 (C), 131.2 (CH), 128.9 (CH), 128.7 (CH), 127.7 (CH), 127.3 (CH), 127.0 (CH), 125.1 (CH), 120.0 (CH), 119.6 (CH_2), 66.4 (CH_2), 66.3 (CH_2), 61.9 (CH), 49.2 (CH_2), 47.3 (CH), 40.0 (CH_2), 37.1 (CH_2), 31.4 (CH_2), 28.2 ($(\text{CH}_3)_3$). HRMS (ESI) m/z : $[\text{M}+\text{Na}]^+$ calculated $\text{C}_{35}\text{H}_{40}\text{N}_2\text{O}_6\text{SNa}$: 639.2505, found: 639.2501.

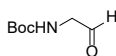
***N*-(2-((Fmoc)amino)ethyl)-*N*-(*tert*-butoxycarbonyl)-*S*-octyl-L-cysteine (14a)**


Allyl *N*-(2-((Fmoc)amino)ethyl)-*N*-(*tert*-butoxycarbonyl)-*S*-octyl-L-cysteinate (**13a**) (289 mg, 0.452 mmol) was dissolved in dry THF (5.0 mL). $\text{Pd}(\text{PPh}_3)_4$ (15.7 mg, 13.5 μ mol, cat.) and *N*-methylaniline (150 μ L, 1.36 mmol, 3.0 eq.) were added and the mixture was stirred for 2 hours while protected from light. The reaction mixture was concentrated *in vacuo*, redissolved in a mixture of EtOAc and petroleum ether (50/50) and washed twice with 1 M aq. NaHCO_3 . The organic layer was then washed with brine, dried over Na_2SO_4 , filtered and concentrated *in vacuo*. The crude product was purified by silica gel column chromatography eluting with 20–40% EtOAc in petroleum ether yielding *N*-(2-((Fmoc)amino)ethyl)-*N*-(*tert*-butoxycarbonyl)-*S*-octyl-L-cysteine **14a** as a white solid (192 mg, 0.320 mmol, 71%). ^1H NMR (400 MHz, CDCl_3) δ 7.95 (s, 2H), 7.76 (d, J = 7.4 Hz, 2H), 7.58 (d, J = 7.5 Hz, 2H), 7.37 (t, J = 7.6 Hz, 2H), 7.33 – 7.26 (m, 2H), 5.95 – 5.81 (m, 1H), 4.61 – 4.29 (m, 2H), 4.28 – 4.13 (m, 1H), 3.94 – 3.71 (m, 1H), 3.63 – 3.36 (m, 2H), 3.35 – 2.99 (m, 2H), 2.59 – 2.45 (m, 2H), 1.60 – 1.48 (m, 2H), 1.48 – 1.37 (m, 9H), 1.37 – 1.17 (m, 10H), 0.87 (t, J = 6.9 Hz, 3H). ^{13}C NMR (101 MHz, CDCl_3) δ 174.3 (C), 144.0 (C), 141.34 (C), 127.8 (CH), 127.2 (CH), 125.3 (CH), 120.1 (CH), 66.9 (CH_2), 61.8 (CH), 47.3 (CH), 33.0 (CH_2), 32.9 (CH_2), 31.9 (CH_2), 29.7 (CH_2), 29.3 (CH_2), 29.0 (CH_2), 28.34 ($(\text{CH}_3)_3$), 22.8 (CH_2), 14.2 (CH_3). HRMS (ESI) m/z : $[\text{M}+\text{Na}]^+$ calculated $\text{C}_{33}\text{H}_{46}\text{N}_2\text{O}_6\text{SNa}$: 621.2975, found: 621.2970.

***N*-(2-((Fmoc)amino)ethyl)-*N*-(*tert*-butoxycarbonyl)-*S*-benzyl-L-cysteine (14b)**


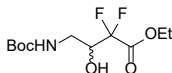
Allyl *N*-(2-((Fmoc)amino)ethyl)-*N*-(*tert*-butoxycarbonyl)-*S*-benzyl-L-cysteinate (**13b**) (176 mg, 0.285 mmol) was dissolved in dry THF (5.0 mL). Pd(PPh₃)₄ (9.88 mg, 8.56 μmol, cat.) and *N*-methylaniline (92.5 μL, 0.855 mmol, 3 eq.) were added and the mixture was stirred for 2 hours while protected from light. The reaction mixture was concentrated *in vacuo*, redissolved in EtOAc and washed with water. The organic layer was then washed with brine, dried over Na₂SO₄, filtered and concentrated *in vacuo*. The crude product was purified by silica gel column chromatography eluting with 20–40% EtOAc in petroleum ether (with 1% AcOH) yielding *N*-(2-((Fmoc)amino)ethyl)-*N*-(*tert*-butoxycarbonyl)-*S*-benzyl-L-cysteine **14b** as a transparent oil (141 mg, 0.244 mmol, 86%). ¹H NMR (400 MHz, CDCl₃) δ 7.75 (d, *J* = 7.7 Hz, 2H), 7.57 (d, *J* = 7.6 Hz, 2H), 7.38 (t, *J* = 7.5 Hz, 2H), 7.32 – 7.26 (m, 6H), 7.25 – 7.19 (m, 1H), 5.69 (br, 1H), 4.54 – 4.28 (m, 2H), 4.27 – 4.14 (m, 1H), 3.70 (d, *J* = 4.4 Hz, 3H), 3.32 (s, 2H), 3.21 – 2.87 (m, 4H), 1.48 – 1.30 (m, 9H). ¹³C NMR (101 MHz, CDCl₃) δ 144.0 (C), 141.4 (C), 129.0 (CH), 128.8 (CH), 127.8 (CH), 127.4 (CH), 127.2 (CH), 125.2 (CH), 120.1 (CH), 66.9 (CH₂), 61.2 (CH), 49.3 (CH₂), 47.3 (CH), 40.0 (CH₂), 37.2 (CH), 31.4 (CH₂), 28.3 ((CH₃)₃). HRMS (ESI) *m/z*: [M+H]⁺ calculated C₃₂H₃₆N₂O₆S: 577.2367, found: 577.2366.

tert-butyl (2-oxoethyl)carbamate (**16**)



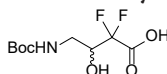
Sodium periodate (**15**) (22.4 g, 105 mmol) was added to a suspension of *tert*-butyl (2,3-dihydroxypropyl) carbamate (10.0 g, 52.3 mmol) in water (250 mL) and the reaction mixture was stirred at room temperature for 1 hour. The aqueous phase was then extracted with MTBE (4 × 250 mL). The combined organic extract was dried over anhydrous Na₂SO₄ and evaporated to dryness to afford *tert*-butyl (2-oxoethyl)carbamate as a golden semisolid oil (7.99 g, 96%) which was used in the next step without any further purification. ¹H NMR (300 MHz, CDCl₃) δ 9.59 (s, 1H), 5.27 (br s, 1H), 4.28 (d, *J* = 5.3 Hz, 2H), 1.46 (s, 9H). ¹³C NMR (75 MHz, CDCl₃) δ 196.5 (C), 154.9 (C), 84.1 (C), 63.3 (CH₂), 27.9 ((CH₃)₃).

ethyl 4-((*tert*-butoxycarbonyl)amino)-2,2-difluoro-3-hydroxybutanoate (**17**)



A solution of *tert*-butyl (2-oxoethyl)carbamate (7.99 g, 50.2 mmol), and ethyl bromodifluoroacetate (13.2 g, 65.3 mmol) in dry THF (150 mL) was added dropwise to a suspension of zinc dust (6.56 g, 100 mmol) in dry THF (100 mL). After complete addition, the reaction was heated to reflux for 2 hours. The reaction mixture was allowed to cool to r.t. and decanted from unreacted zinc. To the reaction mixture was added 1 M KHSO₄ (250 mL) and Et₂O (250 mL). The organic layer was washed with NH₄Cl solution (2 × 250 mL). The organic layer was dried over Na₂SO₄, filtered and concentrated. The product was purified by flash chromatography on silica eluting 5–30% EtOAc in petroleum ether to afford ethyl 4-((*tert*-butoxycarbonyl)amino)-2,2-difluoro-3-hydroxybutanoate as a colourless oil (3.26 g 23%). ¹H NMR (400 MHz, CDCl₃) δ 5.05 (br s, 1H), 4.34 (q, *J* = 7.2 Hz, 2H), 4.16 (dtd, *J* = 16.1, 6.9, 3.4 Hz, 1H), 3.52 (ddd, *J* = 14.8, 6.9, 3.4 Hz, 1H), 3.38 (ddd, *J* = 14.8, 6.9, 3.4 Hz, 1H), 1.43 (s, 9H), 1.35 (t, *J* = 7.2 Hz, 3H). ¹³C NMR (101 MHz, CDCl₃) δ 163.2 (C), 157.5 (C), 114.2 (C), 80.6 (C), 71.7 (CH), 63.2 (CH₂), 40.6 (CH₂), 28.3 ((CH₃)₃), 13.9 (CH₃). HRMS (ESI) *m/z*: [M+Na]⁺ calculated C₁₁H₁₉F₂NO₅Na: 306.1129, found: 306.1125.

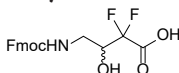
4-((*tert*-butoxycarbonyl)amino)-2,2-difluoro-3-hydroxybutanoic acid (**18**)



Hydrolysis of ethyl ester **1** (0.759 g, 2.68 mmol) to the carboxylic acid was achieved with 1.05 equiv. of 0.25 M LiOH (11.2 mL) in an equal volume to acetonitrile for 2 hours and monitored by TLC. The

mixture was then extracted with ethyl acetate (2×25 mL) to remove byproducts. The aqueous layer was then acidified to pH 2 with 1M HCl and extracted with EtOAc (4×25 mL). The organic layer was dried over Na_2SO_4 and concentrated to afford the carboxylic acid **18** as a colourless oil (521 mg, 76%). ^1H NMR (400 MHz, $\text{DMSO}-d_6$) δ 6.86 (t, $J = 5.8$ Hz, 1H), 6.52 (br s, 1H), 3.97 (dddd, $J = 12.5, 10.1, 8.8, 3.5$ Hz, 1H), 3.23 (ddd, $J = 13.9, 5.8, 3.5$ Hz, 1H), 2.94 (ddd, $J = 13.9, 8.8, 5.8$ Hz, 1H), 1.37 (s, 9H). ^{13}C NMR (101 MHz, $\text{DMSO}-d_6$) δ 170.4 (C), 164.5 (C), 115.1 (C), 77.9 (C), 68.9 (CH), 40.4 (CH_2), 29.1 ($(\text{CH}_3)_3$). HRMS (ESI) m/z : $[\text{M}+\text{H}]^+$ calculated for $\text{C}_9\text{H}_{15}\text{F}_2\text{NO}_5$: 256.0991, found: 256.0988.

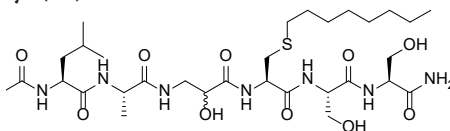
4-((Fmoc)amino)-2,2-difluoro-3-hydroxybutanoic acid (**19**)



4-((*tert*-butoxycarbonyl)amino)-2,2-difluoro-3-hydroxybutanoic acid (485 mg, 1.90 mmol) was deprotected by treatment with a 50:50 (v/v) TFA/DCM solution (30 mL) at r.t. for 2 hours. The TFA/DCM was removed under reduced pressure to afford the TFA salt of the free amine. This was then immediately redissolved in a mixture of aqueous NaHCO_3 (10% w/w, 8 mL) and THF (2 mL). A solution of FmocOSu (0.641 g, 1.90 mmol) in THF (6 mL) was then added and the reaction was stirred overnight until complete. The volatiles were removed under reduced pressure and the remaining solution was treated with 1 M HCl until pH 2 was reached. The aqueous layer was extracted with an equal volume of EtOAc (7 times). The combined organic layer was then washed with brine, dried over Na_2SO_4 filtered and concentrated. The product was purified by flash chromatography on silica gel eluting 0–15% methanol in DCM (supplemented with 1% AcOH) to afford 4-((Fmoc)amino)-2,2-difluoro-3-hydroxybutanoic acid **19** as a white solid (0.672 g, 94%). ^1H NMR (500 MHz, $\text{DMSO}-d_6$) δ 7.88 (dt, $J = 7.5, 0.9$ Hz, 2H), 7.71 (d, $J = 7.5$ Hz, 2H), 7.51 – 7.36 (m, 3H), 7.32 (td, $J = 7.5, 0.9$ Hz, 2H), 6.89 (br s, 1H), 4.27 – 4.18 (m, 3H), 4.05 – 3.89 (m, 1H), 3.30 (ddd, $J = 13.7, 5.8, 3.3$ Hz, 1H), 3.03 (ddd, $J = 14.2, 8.9, 5.8$ Hz, 1H). ^{13}C NMR (126 MHz, $\text{DMSO}-d_6$) δ 165.2 (C), 156.3 (C), 143.9 (C), 140.7 (C), 127.7 (CH), 127.16 (CH), 125.3 (CH), 120.1 (CH), 115.4 (C), 69.7 (CH), 65.6 (CH_2), 46.7 (CH), 41.3 (CH_2). HRMS (ESI) m/z : $[\text{M}+\text{H}]^+$ calculated $\text{C}_{19}\text{H}_{17}\text{F}_2\text{NO}_5$: 378.1148, found: 378.1148.

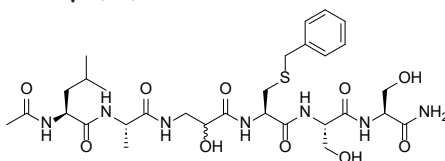
Solid-Phase Peptide Synthesis

Rink Amide MBHA resin was loaded with Fmoc-Ser(*t*Bu)-OH and the resin loading was determined to be $0.378 \text{ mmol g}^{-1}$. Peptides were assembled via standard Fmoc solid-phase peptide synthesis (SPPS) (resin bound AA:Fmoc-AA:BOP:DIPEA, 1:4:4:8 molar eq. for commercially available amino acids, 1:2:2:8 molar eq. for synthetic amino acids) on a 0.1 mmol scale using DMF as solvent. Commercially available amino acids and synthetic amino acids were coupled for 1 and 2 hours, respectively. Fmoc deprotections were carried out with piperidine:DMF (1:4, v/v) for 5 and then 15 minutes. *Tert*-butyl (*t*Bu) was used as a protecting group for serine. Following coupling and Fmoc deprotection of the final amino acid, N-terminal acetylation was achieved by reacting with Ac_2O (resin bound peptide: Ac_2O :pyridine:TEA, 1:5:5:5 molar eq.) for 60 min. Final sidechain deprotection and cleavage from resin was carried out by treatment of the resin with either TFA:TIPS: H_2O :EDT (92.5:2.5:2.5:2.5) for sulphur containing peptides or TFA:TIPS: H_2O (95:2.5:2.5) for all other peptides for 90 min. The reaction mixture was filtered through cotton, and the filtrate precipitated in cold MTBE:petroleum ether (1:1, v/v) and centrifuged (4500 rpm, 5 min). The pellet was then resuspended in MTBE:petroleum ether (1:1, v/v) and centrifuged (4500 rpm, 5 min) and the process repeated an additional two times. Finally the pellet containing the crude peptide was dissolved in $\text{tBuOH}:\text{H}_2\text{O}$ (1:1, v/v) and lyophilised. The crude peptides were purified using preparative HPLC and fractions were checked by HPLC for purity. Pure fractions were combined and lyophilised to yield the desired peptides as white powders. Where possible, peptides were isolated as separate diastereomers identified as 'a' and 'b' unless stated otherwise.

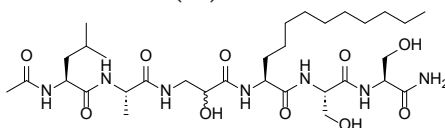
Hydroxymethylcarbonyl-octyl (20)

Diastereomer 1 (20a): Yield: 21.9 mg, 30%. HRMS (ESI) m/z : $[M+H]^+$ calculated $C_{31}H_{57}N_7O_{10}S$: 720.3961, found: 720.3960. R_f HPLC: 16.44 min.

Diastereomer 2 (20b): Yield: 22.4 mg, 31%. HRMS (ESI) m/z : $[M+H]^+$ calculated $C_{31}H_{57}N_7O_{10}S$: 720.3961, found: 720.3965. R_f HPLC: 17.42 min.

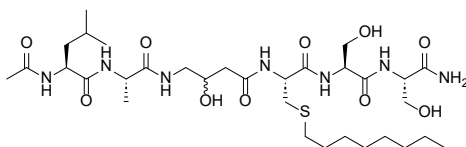
Hydroxymethylcarbonyl-benzyl (21)

The peptide was isolated as a mixture of two diastereomers. Yield: 22.0 mg, 32%. HRMS (ESI) m/z : $[M+H]^+$ calculated $C_{30}H_{47}N_7O_{10}S$: 698.3178, found: 698.3182. HPLC R_f : 13.20 min.

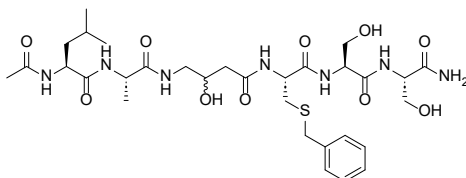
Hydroxymethylcarbonyl-decanoic acid (22)

Diastereomer 1 (22a): Yield: 4.8 mg, 7%. HRMS (ESI) m/z : $[M+H]^+$ calculated $C_{35}H_{55}N_7O_{10}S$: 674.4083, found: 674.4084. R_f HPLC: 15.13 min.

Diastereomer 2 (22b): Yield: 6.7 mg, 10%. HRMS (ESI) m/z : $[M+H]^+$ calculated $C_{35}H_{55}N_7O_{10}S$: 674.4083, found: 674.4088. R_f HPLC: 15.56 min.

Statin-octyl (23)

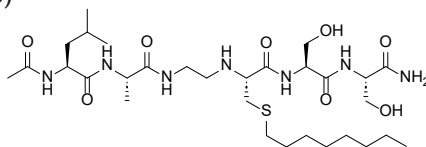
The peptide was isolated as a mixture of two diastereomers. Yield: 31.0 mg, 42%. HRMS (ESI) m/z : $[M+H]^+$ calculated $C_{32}H_{59}N_7O_{10}S$: 734.4117, found: 734.4122. HPLC R_f : 16.75 min.

Statin-benzyl (24)

The peptide was isolated as a mixture of two diastereomers. Yield: 34.0 mg, 48%. HRMS (ESI) m/z :

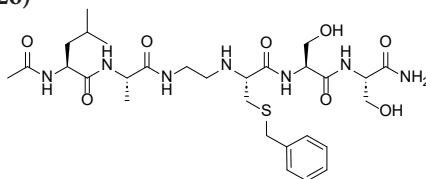
$[M+H]^+$ calculated $C_{31}H_{49}N_7O_{10}S$: 712.3335, found: 712.3341. HPLC R_t : 13.04 min.

Reduced amide-octyl (25)



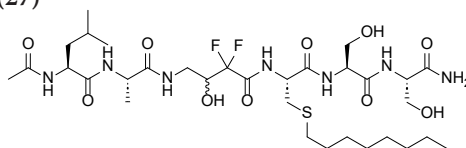
Yield: 7.1 mg 11%. HRMS (ESI) m/z : $[M+H]^+$ calculated $C_{30}H_{57}N_7O_8S$: 676.4062, found: 676.4063. R_t HPLC: 16.43 min.

Reduced amide-benzyl (26)



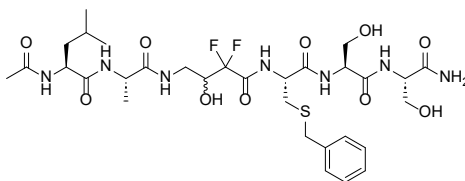
Yield: 6.4 mg, 10%. HRMS (ESI) m/z : $[M+H]^+$ calculated $C_{29}H_{47}N_7O_8S$: 654.3280, found: 654.3283. R_t HPLC: 12.94 min.

Difluoroalcohol-octyl (27)



The peptide was isolated as a mixture of two diastereomers. Yield: 0.85 mg, 1%. HRMS (ESI) m/z : $[M+H]^+$ calculated $C_{32}H_{57}F_2N_7O_{10}S$: 770.3929, found: 770.3928. HPLC R_t : 17.31 min.

Difluoroalcohol-benzyl (28)



DFA-Bn peak 1 (DFA-Bn1): Yield: 1.0 mg, 1%. HRMS (ESI) m/z : $[M+H]^+$ calculated $C_{31}H_{47}F_2N_7O_{10}S$: 748.3146, found: 748.3147. R_t HPLC: 13.71 min.

DFA-Bn peak 2 (DFA-Bn2): Yield: 2.0 mg, 3%. HRMS (ESI) m/z : $[M+H]^+$ calculated $C_{31}H_{47}F_2N_7O_{10}S$: 748.3146, found: 748.3146. R_t HPLC: 13.79 min.

LspA Inhibition Assay

Test compounds were diluted in buffer to $2\times$ final concentration. LspA and FRET substrate were diluted in buffer to $4\times$ their final concentration. Globomycin (500 nM final concentration) was used as a positive control and the negative control wells had no additional compound. The compounds were incubated at 37°C with LspA (12.5 μL , 50 nM final concentration) for 10 mins with shaking every 30 seconds. LspA FRET substrate was then added to the plate (12.5 μL , 7 μM final concentration, 50 μL final volume), before measuring the fluorescence readout at 30 second intervals for 50 minutes at 37°C . Using the initial velocity data of the compounds and the controls, the percentage of LspA inhibited by 500 μM of each compound was calculated. The buffer used was 100 mM MES/NaOH pH 5.4, 150 mM NaCl, 0.05% (w/v) LMNG and the final concentration of DMSO in the experiment was 10 %. Fluorescence readout was measured on a Tecan Spark plate reader (Ex: 320 nm, Em: 420 nm). Microplates used were μClear° , black half-area 96-well plate (Greiner Bio-one).

IC₅₀ Assay

The half-maximal inhibitory concentration (IC₅₀) of each compound was determined against LspA. The compounds were diluted to $2\times$ final concentration and serially diluted (25 μL). The compounds were incubated with LspA (12.5 μL , 50 nM final concentration) for 10 minutes at 37°C , shaking every 30 seconds. LspA FRET substrate (12.5 μL , 7 μM final concentration, 50 μL final volume) was added and fluorescence was measured at 30 second intervals for 50 minutes at 37°C . The initial velocity data was used to produce IC₅₀ curves in GraphPad Prism 7 software. The buffer used was 100 mM MES/NaOH pH 5.4, 150 mM NaCl, 0.05 % (w/v) LMNG and the final concentration of DMSO in the experiment was 10 %. Fluorescence readout was measured on a Tecan Spark plate reader (Ex: 320 nm, Em: 420 nm). Microplates used were μClear° , black half-area 96-well plate (Greiner Bio-one).

MIC Determinations

From glycerol stocks, bacterial strains were cultured on blood agar plates and incubated overnight at 37°C . Following incubation, 3 mL of tryptic soy broth (TSB) was inoculated with an individual colony. The cultures were grown to exponential phase ($\text{OD}_{600} = 0.5$) at 37°C . The bacterial suspensions were then diluted 100-fold in cation-adjusted Mueller–Hinton broth (CAMHB) to reach a bacterial cell density of 10^6 CFU mL^{-1} . In polypropylene 96-well microtiter plates, test compounds were prepared in both regular CAMHB and CAMHB supplemented with polymyxin B nonapeptide (PMBN) to give a final concentration of 8 $\mu\text{g mL}^{-1}$. These solutions were then 2-fold serially diluted to achieve a final volume of 50 μL per well. An equal volume of bacterial suspension (10^6 CFU mL^{-1}) was added to the wells. The plates were sealed with breathable membranes and incubated at 37°C for 18 hours with constant shaking (600 rpm). MICs were determined by visual inspection as the median of a minimum of triplicates.

Acknowledgements

We thank Martijn de Ruiter and Kirsty Arnott for their contributions relating to chemical synthesis, Nicola Wade and Meg Ferguson for synthesising the FRET substrate, Nicola Wade for performing the FRET assays, and Paolo Innocenti for acquiring the HRMS data. Thanks also to Jaco Slingerland for enzymatically obtaining PMBN.

Referenced Works

- 1 C. J. Murray, K. S. Ikuta, F. Sharara, L. Swetschinski, G. Robles Aguilar, A. Gray, C. Han, C. Bisignano, P. Rao, E. Wool, S. C. Johnson, A. J. Browne, M. G. Chipeta, F. Fell, S. Hackett, G. Haines-Woodhouse, B. H. Kashef Hamadani, E. A. P. Kumaran, B. McManigal, R. Agarwal, S. Akech, S. Albertson, J. Amuasi, J. Andrews, A. Aravkin, E. Ashley, F. Bailey, S. Baker, B. Basnyat, A. Bekker, R. Bender, A. Bethou, J. Bielicki, S. Boonkasidecha, J. Bukosia, C. Carvalho, C. Castañeda-Orjuela, V. Chansamouth, S. Chaurasia, S. Chiurchiù, F. Chowdhury, A. J. Cook, B. Cooper, T. R. Cressey, E. Criollo-Mora, M. Cunningham, S. Darboe, N. P. J. Day, M. De Luca, K. Dokova, A. Dramowski, S. J. Dunachie, T. Eckmanns, D. Eibach, A. Emami, N. Feasey, N. Fisher-Pearson, K. Forrest, D. Garrett, P. Gastmeier, A. Z. Giref, R. C. Greer, V. Gupta, S. Haller, A. Haselbeck, S. I. Hay, M. Holm, S. Hopkins, K. C. Iregbu, J. Jacobs, D. Jarovsky, F. Javanmardi, M. Khorana, N. Kissoon, E. Kobeissi, T. Kostyanov, F. Krapp, R. Krumkamp, A. Kumar, H. H. Kyu, C. Lim, D. Limmathurotsakul, M. J. Loftus, M. Lunn, J. Ma, N. Mturi, T. Munera-Huertas, P. Musicha, M. M. Mussi-Pinhata, T. Nakamura, R. Nanavati, S. Nangia, P. Newton, C. Ngoun, A. Novotney, D. Nwakanma, C. W. Obiero, A. Olivas-Martinez, P. Oliaro, E. Ooko, E. Ortiz-Brizuela, A. Y. Peleg, C. Perrone, N. Plakkal, A. Ponce-de-Leon, M. Raad, T. Ramdin, A. Riddell, T. Roberts, J. V. Robotham, A. Roca, K. E. Rudd, N. Russell, J. Schnall, J. A. G. Scott, M. Shivamallappa, J. Sifuentes-Osornio, N. Steenkeste, A. J. Stewardson, T. Stoeva, N. Tasak, A. Thairakong, G. Thwaites, C. Turner, P. Turner, H. R. van Doorn, S. Velaphi, A. Vongpradith, H. Vu, T. Walsh, S. Waner, T. Wangrangsimaikul, T. Wozniak, P. Zheng, B. Sartorius, A. D. Lopez, A. Stergachis, C. Moore, C. Dolecek and M. Naghavi, *Lancet*, 2022, **399**, 629–655.
- 2 J. A. Al-Tawfiq, H. Momattin, A. Y. Al-Ali, K. Eljaaly, R. Tirupathi, M. B. Haradwala, S. Areti, S. Alhumaid, A. A. Rabaan, A. Al Mutair and P. Schlagenhauf, *Infection*, 2022, **50**, 553–564.
- 3 A. H. Delcour, *Biochim. Biophys. Acta*, 2009, **1794**, 808–816.
- 4 H. Nikaido and M. Vaara, *Microbiol. Mol. Biol. Rev.*, 2002, **67**, 593–656.
- 5 H. Nikaido, *Drug Resist. Updat.*, 1998, **1**, 93–98.
- 6 T. J. Silhavy, D. Kahne and S. Walker, *Cold Spring Harb. Perspect. Biol.*, 2010, **2**, a000414.
- 7 W. R. Zückert, *Biochim. Biophys. Acta - Mol. Cell Res.*, 2014, **1843**, 1509–1516.
- 8 N. Buddelmeijer, *FEMS Microbiol. Rev.*, 2015, **39**, 246–261.
- 9 T. El Arnaout and T. Soulimane, *Trends Biochem. Sci.*, 2019, **44**, 701–715.
- 10 M. Wiktor, D. Weichert, N. Howe, C. Y. Huang, V. Olieric, C. Boland, J. Bailey, L. Vogeley, P. J. Stansfeld, N. Buddelmeijer, M. Wang and M. Caffrey, *Nat. Commun.*, 2017, **8**, 25–28.
- 11 L. Vogeley, T. El Arnaout, J. Bailey, P. J. Stansfeld, C. Boland and M. Caffrey, *Science*, 2016, **351**, 876–880.
- 12 S. Kitamura, A. Owensby, D. Wall and D. W. Wolan, *Cell Chem. Biol.*, 2018, **25**, 301–308.e12.
- 13 M. Nakajima, M. Inukai, T. Haneishi, A. Terahara, M. Arai, T. Kinoshita and C. Tamura, *J. Antibiot. (Tokyo)*, 1978, **31**, 426–432.
- 14 K. Gerth, H. Irschik, H. Reichenbach and W. Trowitzsch, *J. Antibiot. (Tokyo)*, 1982, **35**, 1454–1459.
- 15 M. Inukai, M. Takeuchi, K. Shimizu and M. Arai, *J. Antibiot. (Tokyo)*, 1978, **31**, 1203–1205.
- 16 M. Tokunaga, H. Tokunaga and H. C. Wu, *Proc. Natl. Acad. Sci. U. S. A.*, 1982, **79**, 2255–2259.

- 17 M. Hussain, S. Ichihara and S. Mizushima, *J. Biol. Chem.*, 1980, **255**, 3707–3712.
- 18 L. J. Zwiebel, M. Inukai, K. Nakamura and M. Inouye, *J. Bacteriol.*, 1981, **145**, 654–656.
- 19 K. Garland, H. Pantua, M. G. Braun, D. J. Burdick, G. M. Castaneda, Y. C. Chen, Y. X. Cheng, J. Cheong, B. Daniels, G. Deshmukh, Y. Fu, P. Gibbons, S. L. Gloor, R. Hua, S. Labadie, X. Liu, R. Pastor, C. Stivala, M. Xu, Y. Xu, H. Zheng, S. B. Kapadia and E. J. Hanan, *Bioorg. Med. Chem. Lett.*, 2020, **30**, 127419.
- 20 S. Olatunji, X. Yu, J. Bailey, C. Y. Huang, M. Zapotoczna, K. Bowen, M. Remškar, R. Müller, E. M. Scanlan, J. A. Geoghegan, V. Olieric and M. Caffrey, *Nat. Commun.*, DOI:10.1038/s41467-019-13724-y.
- 21 A. K. Ghosh, H. L. Osswald and G. Prato, *J. Med. Chem.*, 2016, **59**, 5172–5208.
- 22 H. V. Motwani, M. De Rosa, L. R. Odell, A. Hallberg and M. Larhed, *Eur. J. Med. Chem.*, 2015, **90**, 462–490.
- 23 A. M. Silva, R. E. Cachau, H. L. Sham and J. W. Erickson, *J. Mol. Biol.*, 1996, **255**, 321–340.
- 24 A. T. Neffe, M. Bilang and B. Meyer, *Org. Biomol. Chem.*, 2006, **4**, 3259–3267.
- 25 H. Abdel-Rahman, G. Al-karamany, N. El-Koussi, A. Youssef and Y. Kiso, *Curr. Med. Chem.*, 2012, **9**, 1905–1922.
- 26 A. Brik and C. H. Wong, *Org. Biomol. Chem.*, 2003, **1**, 5–14.
- 27 K. Ersmark, B. Samuelsson and A. Hallberg, *Med. Res. Rev.*, 2006, **26**, 626–666.
- 28 C. L. Moore, D. D. Leatherwood, T. S. Diehl, D. J. Selkoe and M. S. Wolfe, *J. Med. Chem.*, 2000, **43**, 3434–3442.
- 29 N. I. Martin, J. J. Woodward, M. B. Winter and M. A. Marletta, *Bioorg. Med. Chem. Lett.*, 2009, **19**, 1758–1762.
- 30 S. Giovani, M. Penzo, S. Brogi, M. Brindisi, S. Gemma, E. Novellino, L. Savini, M. J. Blackman, G. Campiani and S. Butini, *Bioorganic Med. Chem. Lett.*, 2014, **24**, 3582–3586.
- 31 T. Van Kersavond, R. Konopatzki, M. A. T. van der Plassche, J. Yang and S. H. L. Verhelst, *RSC Adv.*, 2021, **11**, 4196–4199.
- 32 S. Kitamura and D. W. Wolan, *FEBS Lett.*, 2018, **592**, 2289–2296.
- 33 Umezawa H., T. Aoyagi, H. Morishima, M. Matsuzaki, M. Hamada and T. Takeuchi, *J. Antibiot. (Tokyo)*, 1970, **23**, 259–262.
- 34 R. A. Dixon and I. Chopra, *J. Antimicrob. Chemother.*, 1986, **18**, 557–563.

Supplementary Figures

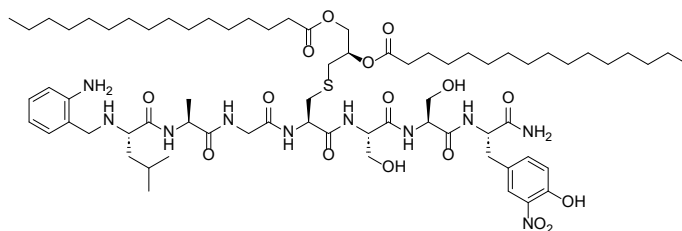


Figure S1. The structure of the FRET substrate used in the LspA activity assays. Synthesised by Nicola Wade and Meg Ferguson.

Table S1. *In vitro* minimum inhibitory concentrations (MIC) of peptidomimetic LspA inhibitors. Assays were conducted in CAMHB in both the absence and presence of 8 µg/mL PMBN.

Compound	MIC (µg mL ⁻¹)				MIC with 8 µg/mL PMBN (µg mL ⁻¹)			
	E.C.	K.P.	A.B.	P.A.	E.C.	K.P.	A.B.	P.A.
20a	>64	>64	>64	>64	>64	>64	>64	>64
20b	>64	>64	>64	>64	>64	>64	>64	>64
21	>64	>64	>64	>64	>64	>64	>64	>64
22a	>64	>64	>64	>64	>64	>64	>64	>64
22b	>64	>64	>64	>64	>64	>64	>64	>64
23	>64	>64	>64	>64	>64	>64	>64	>64
24	>64	>64	>64	>64	>64	>64	>64	>64
25	>64	>64	>64	>64	>64	>64	>64	>64
26	>64	>64	>64	>64	>64	>64	>64	>64
27	>64	>64	>64	>64	>64	>64	>64	>64
28a	>64	>64	>64	>64	>64	>64	>64	>64
28b	>64	>64	>64	>64	>64	>64	>64	>64
Polymyxin B	2	1	0.25	2	-	-	-	-
PMBN	>64	>64	>64	>64	-	-	-	-

E.C. = *E. coli* ATCC 25922, K.P. = *K. pneumoniae* NCTC 11228, A.B. = *A. baumannii* ATCC 17961, P.A. = *P. aeruginosa* ATCC 10145, PMBN = polymyxin B nonapeptide.